The epigenetic regulators CBP and p300 facilitate leukemogenesis and represent therapeutic targets in Acute Myeloid Leukemia

George Giotopoulos[1,2*], Wai-In Chan[1,2,3*], Sarah J. Horton[1,2], David Ruau[1,2], Paolo Gallipoli[1,2], Alexis Fowler[1], Charles Crawley[1], Elli Papaemmanuil[4], Peter J. Campbell[1,4], Berthold Göttgens[1,2], Jan M. Van Deursen[5], Philip A. Cole[6], Brian J.P. Huntly[1,2].

1. Department of Haematology, Cambridge Institute for Medical Research and Addenbrookes Hospital, University of Cambridge, Cambridge, CB2 0XY, UK
2. Wellcome Trust - Medical Research Council Cambridge Stem Cell Institute
3. State Key laboratory of Quality Research in Chinese Medicine, Macau University of Science and Technology, Avenida Wai Long, Taipa, Macau.
4. Wellcome Trust Sanger Institute, Hinxton, CB10 1SA, UK
5. Department of Pediatric and Adolescent Medicine, Mayo Clinic College of Medicine, Rochester, Minnesota, 55905
6. Department of Pharmacology and Molecular sciences, Johns Hopkins School of Medicine, 725 N. Wolfe St., Baltimore, MD, 21205

* These authors contributed equally to this work

Running Title: CBP/EP300 as therapeutic targets in AML

The authors declare no conflict of interest.

Funding came from: Cancer Research UK, Leukaemia Lymphoma Research, the Kay Kendal Leukaemia Fund, the Leukemia lymphoma Society of America, the Wellcome Trust, The Medical Research Council and NIHR Cambridge Biomedical Research Centre.

Corresponding Author: Dr Brian Huntly, Email – bjph2@cam.ac.uk ; Phone: +44 (0) 1223 331153; Fax: +44 (0) 1223 762670

Word count: 4497, Figures: 6

Abstract

Growing evidence links abnormal epigenetic control to the development of hematological malignancies. Accordingly, inhibition of epigenetic regulators is emerging as a promising therapeutic strategy. The acetylation status of lysine residues in histone tails is one of a number of epigenetic post-translational modifications that alter DNA-templated processes, such as transcription, to facilitate malignant transformation. Although histone deacetylases are already being clinically targeted, the role of histone lysine acetyltransferases (KAT) in malignancy is less well characterised. We chose to study this question in the context of acute myeloid leukemia (AML), where, using *in vitro* and *in vivo* genetic ablation and knockdown experiments in murine models, we demonstrate a role for the epigenetic regulators CBP and p300 in the induction and maintenance of AML. Furthermore, using selective small molecule inhibitors of their lysine acetyltransferase activity, we validate CBP/p300 as therapeutic targets *in vitro* across a wide range of human AML subtypes. We proceed to show that growth retardation occurs through the induction of transcriptional changes that induce apoptosis and cell cycle arrest in leukemia cells and finally demonstrate the efficacy of the KAT inhibitors to decrease clonogenic growth of primary AML patient samples. Taken together, these data suggest that CBP/p300 are promising therapeutic targets across multiple subtypes in AML.

Keywords: AML, epigenetic regulators, small molecule inhibitors.

Introduction.

Acute Myeloid Leukemia (AML) is an often fatal hematological malignancy[1] characterised by abnormal transcriptional programs and driven by a plethora of heterogeneous mutations.[2] A central and recurrent theme is mutation of epigenetic regulators.[3] Amongst these are the transcriptional co-activators cyclic-AMP response element binding protein (CREB)-binding protein (CREBBP or KAT3A, hereafter referred to as CBP) and its paralogue EP300 (KAT3B, hereafter referred to as p300). CBP and p300 modulate locus-specific transcription via a number of separate mechanisms.[4] These include direct lysine acetyltransferase (KAT) catalytic activity, where CBP and p300 can acetylate both histone and non-histone proteins[5], as well as through multiple protein-protein interactions between CBP or p300 and transcription factors, chromatin remodelling complexes and the basal transcriptional machinery.[6] *Cbp* and *p300* are required during development for the generation and function of normal hematopoietic stem cells (HSC)[7] and we have recently shown that *Cbp* is also required for adult HSC maintenance and function.[8] Recently, inactivating mutations in *CBP* and *p300* have been described in a number of hematological malignancies[9-11] and this, together with the description of germline mutations of CBP in the cancer predisposition syndrome Rubinstein-Taybi syndrome[12] and of hematological malignancies in *Cbp* deficient mice[8, 13], identify CBP and p300 as tumour suppressor genes. However, in AML, there have been reports of rearrangements of both *CBP* and *p300* with the mixed lineage leukemia (*MLL*) gene and of *CBP* with the *MOZ (MYST3*) gene, all leading to the generation of leukemogenic fusion proteins.[14-15] Additionally, many oncogenes have been demonstrated to interact with CBP, including the oncogenic fusions MOZ-TIF2 and NUP98-HOXA9, MLL-AFX and TCF3-PBX.[16-19] Furthermore, structure function analysis of these fusions has demonstrated that removal of the protein domains that interact with CBP abrogates transformation.[16-17] These apparently counterintuitive data suggest that CBP and p300 may also function as oncogenes, as has been described for other tumour suppressor genes[20], and facilitate transformation in certain types of AML.

AML remains a disease with an overall dismal outlook, with over 70% of patients eventually succumbing to the disease.[21] In addition, the mainstays of AML therapy are unchanged for the last 20 years.[1] Therefore, novel therapeutics are urgently required to improve the long-term outlook in this aggressive disease. To this end, agents targeting epigenetic regulators, particularly those with catalytic function, such as DNA methyltransferases and histone deacetylase inhibitors, have recently been used with some success in AML and other hematological malignancies.[22] In addition, we and others have recently targeted so called "epigenetic readers"[3], through the inhibition of protein-protein interactions between acetylated histone tails and the BET protein family of transcriptional activators.[23] However, the role of histone acetyltransferase activity has not been systematically investigated, nor targeted in AML. In this report, we support this strategy by demonstrating that *Cbp* and *p300* are genetically required for efficient leukemogenesis. Moreover, we demonstrate that pharmacologically targeting the catalytic activity of the lysine acetyltransferases (KAT) CBP and p300 has pre-clinical efficacy in many subtypes of AML. This occurs via the induction of cell cycle arrest and apoptosis, whilst sparing normal hematopoietic progenitors in similar assays. Mechanistically, cell cycle arrest and apoptosis appear to be mediated through alteration of a transcriptional program associated with genomic integrity. Finally we demonstrate a significant decrement of clonogenic growth in AML patient samples following CBP/p300 KAT inhibition. Taken together, these data suggest targeting CBP/p300 activity as a promising clinical strategy in AML.

Results.

Cbp is required for efficient immortalization *in vitro* and induction and maintenance of AML *in vivo.*

To assess the requirement for *Cbp* during transformation, we retrovirally transduced c-kit$^+$ bone marrow (BM) cells from *Cbpfl/fl;Mx1-Cre*$^-$ mice (hereafter *Cbp* wt) or *Cbpfl/fl;Mx1-Cre*$^+$ mice following administration of poly-I poly-C (pIpC) (hereafter *Cbp*$^{-/-}$), with AML-associated oncogenes *MOZ-TIF2* (MT2) or *NUP98-HOXA9* (NHA9), both of which are known to interact with CBP. Transformation was assessed in standard serial replating and growth in liquid culture assays[24]. No differences in colony numbers or growth were demonstrated between MT2 and NHA9 *Cbp* wt or *Cbp*$^{-/-}$ progenitor cells (Figure 1A), suggesting that *in vitro* immortalization by MT2 and NHA9 is not absolutely dependent on *Cbp* expression, and may proceed in its absence. We next examined if *Cbp* is required for continued *in vitro* self-renewal in cell lines expressing MT2 and NHA9. *Cbpfl/fl* c-kit$^+$ progenitor cells were first transduced with either MT2 or NHA9 and serially replated in methylcellulose. Similar cells expressing *MLL-ENL* (ME), a fully transforming fusion protein not documented to interact with CBP, were included as a control. Following the third round of plating, cells were transduced with pBabe-Cre-puro retrovirus to excise *Cbp in vitro*, or with a puro-empty vector as control, prior to further serial plating under initial puromycin selection. Although transduction with Cre recombinase did not significantly alter the self-renewal potential in any cell line at the population level (Figure 1B and data not shown), genotyping of the cells revealed preferential growth by cells that lacked recombination and therefore still expressed Cbp, demonstrating its involvement in transformation. Importantly, by the 3rd and 4th round of plating, almost all cells immortalized by NHA9 and MT2 demonstrated the non-recombined allele, suggesting a selective advantage for cells that retained Cbp (Figure 1C). In contrast, cells expressing ME demonstrated efficient and sustained excision of *Cbp* (Figure 1C and data not shown). Taken together, these strongly suggest that loss of *Cbp* may affect the self-renewal programs maintained by oncogenes that interact with it, including MT2 and NHA9, but not by those that do not interact with Cbp, as exemplified by ME.

We next assessed the requirement for *Cbp* during the initiation and maintenance of leukemia *in vivo*, using the short latency MT2 AML model.[16, 24] To test the requirement for *Cbp* during leukemia initiation, c-kit$^+$ BM cells from previously pIpC treated *Cbp* wt or *Cbp*$^{-/-}$ mice were transduced with MSCV-MT2-IRES-GFP (Figure 2A). The transduction efficiency between *Cbp* wt and *Cbp*$^{-/-}$ cells (as measured by the percentage of GFP$^+$ cells) was similar and genotyping of the transduced cells revealed excision of the *Cbp* allele (Figure 2A) before transplantation. All MT2 mice succumbed to disease within 2-4 months after transplantation, with a similar macroscopic and histological AML phenotype (Figure 2A & Supplementary Figure 1). However, similarly to the findings *in vitro*, genotyping from various heavily infiltrated tissues of the leukemic mice from the *Cbp*$^{-/-}$ group demonstrated that the majority of cells actually retained the non-recombined *Cbpfl/fl* allele and therefore expressed *Cbp*. Indeed, when these populations were enriched for leukemic cells, by sorting for GFP, all cells lacked recombination at the *Cbp* allele (Figure 2A). Thus, in agreement with our *in vitro* studies, there is a significant growth advantage during leukemia induction for cells that continue to express *Cbp*.

We next examined if *Cbp* is required for maintenance of leukemia. c-kit$^+$ BM cells were isolated from *Cbpfl/fl;Mx1-Cre*$^+$ mice (not previously treated with pIpC). These cells were transduced with MSCV-MT2-IRES-GFP and transplanted into lethally irradiated recipient mice (Figure 2B). Leukemic cells were harvested from primary mice and further transplanted into sub-lethally irradiated secondary recipients. Five doses of pIpC were administered to half of the recipient mice, starting at 10 days post-transplantation to allow for proper engraftment, with control mice receiving no treatment. Mice from the untreated group succumbed to disease between 19-35 days later (Figure 2B). By contrast, only 40% of the mice from the pIpC treated group died from disease, although they did so with a similar latency. In the remaining pIpC treated mice, no GFP positive cells could be detected in the peripheral blood on serial testing, nor were *Cbpfl/fl* or recombined alleles detected by genotyping and no disease was evident at the termination of the experiment on day 120 (Figure 2B and data not shown). Thus, similarly

to our *in vitro* replating assays, loss of *Cbp in vivo* compromises effective induction and maintenance of MT2-associated AML.

Functional redundancy exists between Cbp and p300 during myeloid transformation.

Cbp and its closely related paralogue *p300* have similar, but also unique functions.[7] We hypothesised that p300 may partially compensate for Cbp loss and explain why Cbp was not an absolute requirement for immortalisation *in vitro*. To test this hypothesis we knocked down *p300*, using two lentiviral shRNAs (sh747 and sh1945) in *Cbp* wt and *Cbp*$^{-/-}$ cells immortalized by MT2 or NHA9. Modest knockdown (up to 60% of mRNA, sh747, Figure 3A) of *p300* in *Cbp* wt MT2 expressing cells decreased the numbers of colonies in methylcellulose culture, in comparison to cells expressing a control shRNA construct that targets luciferase (Figure 3B). This decrease was even more marked in *Cbp*$^{-/-}$ cells (Figure 3B), with similar results also demonstrated in the NHA9 cell line (Figure 3B). Taken together, our data suggest functional redundancy between Cbp and p300, which cooperate to facilitate the maintenance of self-renewal programs in cells immortalized by the AML-associated fusion proteins MT2 and NHA9.

Inhibition of the KAT activity of CBP/p300 suppresses the growth of multiple AML subtypes through the induction of cell cycle arrest and apoptosis.

In order to bypass the functional redundancy between Cbp and p300 and to determine whether other subtypes of AML also require CBP/p300, we employed a pharmacological strategy that utilized a highly selective small molecule inhibitor of CBP and p300 KAT activity, C646[25] (Supplementary Figure 2A). Initially, all experiments were conducted with both an inactive structural analogue of C646, C37, and vehicle control (DMSO), but as responses to C37 and DMSO were identical, we continued only with DMSO as a control (Supplementary Figure 2B and data not shown). We first demonstrated that C646 treatment was not associated with any significant toxicity to normal murine hematopoietic stem and progenitor cells in colony formation, colony composition and in serial replating assays up to a dosage of 30uM (Figure 4A and data not shown). All subsequent assays were therefore performed at a dosage

of 20uM. At this dosage, we demonstrated significant inhibition of growth for MT2 and NHA9 immortalized cell lines in liquid culture and in methylcellulose colony assays (Figure 4B and Supplementary Figure 3A). We extended this analysis to a panel of human AML cell lines representative of common oncogenic driver mutations (Figure 4C and Supplementary Table 1). Growth rates for 10 separate cell lines were assessed in liquid culture assays (DMSO *vs.* C646). As demonstrated in Figure 4C, 8 cell lines demonstrated a significant reduction in growth, with 7/10 cell lines demonstrating a greater than 50% reduction in growth in liquid culture following C646 treatment. Similarly, in methylcellulose assays, colony growth was significantly reduced in 8/10 and by greater than 50% in 5/10 cell lines (Figure 4D). Taken together, these results demonstrate significant efficacy for CBP/p300 KAT inhibition across a number of AML subtypes.

To further determine the cellular consequences of KAT inhibition, we performed apoptosis and cell cycle analysis post-C646 treatment. Inhibition with C646 was associated with a variable induction of apoptosis at 72hours (Figure 4E and Supplementary Figure 3C). There was no induction of apoptosis in normal human $CD34^+$ cells in liquid culture at similar dosage (Figure 6B). A modest alteration of cell cycle was observed with induction of G_1/G_0 arrest in the responsive, but not the resistant cell lines (Figure 4F).

Inhibition of CBP/p300 lysine acetyltransferase (KAT) activity in human leukemia cells alters a transcriptional programme associated with genomic integrity.

To determine the critical transcriptional programs altered in AML cells that mediate cell cycle arrest and cell death, we analysed global gene expression patterns following treatment with C646 or DMSO control, in two sensitive (Kasumi-1 and KG-1) and one resistant (K562) cell lines. Gene expression was assessed 24hours post-treatment, a time point prior to the induction of significant apoptosis or cell cycle alteration (Supplementary Figure 4). Significant differential gene expression changes (FDR <5%; FD: +/- 1.5-fold (Log_2 scale)) were noted for 348 and 231 genes in the sensitive cells lines KG1 and

Kasumi-1, respectively and for 47 genes for the resistant cell line K562 (Figure 5A). There was a high correlation between the deregulated genes in the two sensitive cell lines (KG1 and Kasumi-1, ($p < 2.2^{-16}$) (Figure 5B) suggesting that KAT inhibition generates specific rather than general transcriptional changes. Ninety-eight genes were commonly differentially expressed in the two sensitive cell lines. To further prioritise gene expression changes associated with sensitivity to C646, 11 genes that were also differentially expressed in the resistant cell line K562 were subtracted from this gene list (Figure 5C). When the GO terms for the remaining 87 genes (57 genes downregulated and 30 genes upregulated, Figure 5D and Supplementary Table 2) were examined, there was significant enrichment for genes involved in DNA replication, DNA repair, the control of mitosis and the cell cycle (Figure 5D). Moreover, 43% (38/87) of these genes have been previously identified as direct p300 targets (p300 ChIP data from the ENCODE project[26], Supplementary Table 2). In agreement with the histone acetyltransferase function of CBP/P300, transcriptional repression was accompanied by reduced H3K18Ac levels in the promoter region of selected candidate genes, as validated by ChIP-PCR (Figure 5E) 24hours post-KAT inhibition. The differential (and sensitive cell line-specific) expression pattern fits well with the cellular consequences observed following HAT inhibition. These findings are also in agreement with previous observations of a cell cycle defect upon *Cbp* deletion in normal hematopoietic stem and progenitor cells.[8] GSEA analysis corroborated that DNA replication and cell cycle progression are affected upon KAT inhibition, as the treated *vs.* untreated profiles were significantly enriched for genes involved in those processes (Supplementary Figure 5).

CBP/p300 KAT inhibitors decrease growth of primary human AML samples.

Finally, the efficacy of KAT inhibition was tested in primary human AML samples. Importantly, no evidence of C646 toxicity to normal $CD34^+$ cells was seen in methylcellulose or apoptosis assays (Figure 6A and B). However, in primary blasts from a large set of AML patients a markedly different pattern was demonstrated. C646 was tested on twenty-nine AML cases harbouring a number of differing molecular and cytogenetic abnormalities. Similar to the effects seen in AML cell lines, a significant reduction in

clonogenic potential was demonstrated in the majority of patient samples (p= 0.0004, Figure 6C). Indeed, 65% of samples (19/29) across a number of AML molecular subtypes, including those associated with a poor prognosis, demonstrated a significant (>50%) reduction in colony number (Figure 6D & Supplementary Figure 6).

Discussion.

Survival rates for AML patients are dismal, with over 70% of patients eventually succumbing to the disease. This statistic has not been helped by the recent lack of novel therapeutics developed for AML. Agents with efficacy against specific molecular subtypes, including ATRA for acute promyelocytic leukemia (APML)[23], the toxin-conjugated anti-CD33 antibody Myelotarg for core-binding factor mutated AML[27] and FLT3 inhibitors for patients with activating FLT3 mutations[28] have shown promising effects in specific subtypes of AML. However, agents with effects against a wider number of AML subtypes have failed to emerge. Recently, inhibitors of epigenetic regulators have demonstrated promise in hematopoietic malignancies. In this report, we present data supporting the role of the epigenetic regulators CBP/p300 in AML pathogenesis and, using pharmacological inhibition of their KAT activity in preclinical studies identify these proteins as therapeutic targets across a wide range of AML subtypes.

Our genetic experiments using *in vitro* and *in vivo* murine models of leukemia were strongly suggestive of a *Cbp* role in AML induction and maintenance. This was further supported by our shRNA assays, which suggested and addressed the compensatory role of p300 following *Cbp* loss. In order to bypass the limitations of these genetic approaches and therapeutically validate these results, we utilized a small molecule inhibitor that specifically targets both CBP and p300 KAT activity, thus allowing dissection of the relative roles of their catalytic activity and their non-catalytic protein scaffold functions in leukemogenesis. We encountered no evidence of toxicity to normal haematopoiesis (murine and human cells) in our *in vitro* assays. This is in keeping with the mild hematopoietic phenotype we observed *in vivo* under homeostatic conditions following acute *Cbp* deletion.[8] Of note, the hematopoietic phenotype of mice carrying a KAT defective mutant of p300 is minimal, whereas mice with a p300 KIX-domain mutant allele, predicted to abrogate multiple protein-protein interactions, demonstrate a marked hematopoietic phenotype.[29]

Also supportive of a lack of general toxicity were the specific gene expression changes observed following treatment. Pharmacological inhibition of CBP and p300, affected specific and partially overlapping programs in two sensitive cell lines. Many of these differentially expressed genes are involved in DNA integrity and cell cycle control. These alterations are in keeping with the proposed role of CBP and p300 in other DNA-templated processes, including repair, replication and recombination.[30] In particular, multiple members of the minichromosome maintenance pre-replication complex (MCM3, MCM4 and MCM5), as well as its interacting proteins (MCM10) and loading/regulatory factors for replication origin licensing (CDT1 and GMNN) were downregulated in sensitive, but not resistant cell lines. These data would also, at least partially, explain the observed altered cellular phenotype of cell cycle arrest and apoptosis.

Although the exact mechanism(s) whereby CBP and p300 inhibition alter transcription in AML remains unknown, a number of non-mutually exclusive mechanisms could be envisaged. CBP and p300 are known to interact with multiple hematopoietic transcription factors and also with known oncogenes, therefore inhibition of direct co-activator function for driver oncogenes may underlie effects in certain AML subtypes. Our genetic experiments in MOZ-TIF2 and NUP98-HOXA9 support this, as do reports of the efficacy in acute leukemias of small molecule inhibitors that directly target the interaction between CBP and/or p300 and β-Catenin[31] and the observation that nearly half of the differentially expressed genes following CBP/P300 KAT inhibition are direct targets of p300, as shown by ChIP-Seq data deposited in the ENCODE database. Another possibility is that these inhibitors target CBP and p300 co-activator activity at critical transcriptional mediators downstream of oncogenic mutations. Finally, lysine acetylation of non-histone proteins mediated by CBP and/or p300 has been suggested to facilitate leukemogenesis. In support of this concept, targeting KAT activity in AML1-ETO positive leukemia cells led to decreased leukemia growth associated with decreased site-specific AML1-ETO acetylation.[32] Furthermore, AML1-ETO proteins mutated to prevent site-specific acetylation were poorly transforming *in vivo* and AML1-ETO positive patient samples and cell lines are sensitive to

CBP/p300 inhibition.[33] Thus acetylation of both histone and non-histone proteins by CBP and p300 may facilitate leukemogenesis. Further investigations are warranted, therefore, to address the specific role of these mechanisms in transformation in individual AML subtypes.

Unfortunately, the C646 HAT inhibitor lacks sufficient potency and shows unfavorable pharmacokinetic properties (unpublished data) to allow effective dosing *in vivo*. However, *Cbp* ablation *in vivo* significantly impeded leukemic growth. In addition, the majority of AML cell lines and most AML patient samples, including those with a number of poor risk genetic characteristics (including FLT3-ITD, TP53, DNMT3A, TET2, and ASXL1 mutations and EVI-1 and TP53 rearrangements, as documented by directed NGS in some patients, Figure 6D), demonstrated a significant decrease in clonogenic growth upon inhibitor treatment *in vitro*. Importantly, no significant toxicity was seen in normal murine and human hematopoietic cells treated with the same dose of inhibitor. Taken together, our *in vivo* genetic data and pharmacological *in vitro* data suggest promising efficacy in targeting CBP and p300 function in AML. Therefore, novel potent and specific agents, optimised for *in vivo* use, are urgently required to validate the promising efficacy and lack of toxicity of CBP/p300 KAT inhibition, and to move this potential treatment paradigm towards clinical testing in AML. However, as a note of caution, if efficacy is demonstrated, due to the association of CBP and p300 loss with tumour induction and a chemo-resistant phenotype[9-11], caution will be warranted as to how CBP/p300 inhibitors can best be integrated into combination therapies for AML.

Materials and methods.

Retroviral transduction assays. Retroviral transduction protocols and constructs (MSCV-NUP98-HOXA9-neo, MSCV-NUP98-HOXA9-IRES-GFP, MSCV-MOZ-TIFF2-neo and MSCV-MOX-TIFF2-IRES-GFP) have been previously described[10]. Cre cDNA was subcloned into a pBabe-puro vector. Bone marrow cells were harvested from 6-8 week old *Cbpfl/fl*;wt(wt) or *Cbpfl/fl*;Mx(Mx) mice that had been treated with 5 doses of pIpC (Sigma;300ug/dose). c-kit$^+$ BM cells were selected using CD117MicroBeads (Miltenyi Biotec). For the serial replating assays, 10^4 transduced cells were plated in duplicate in methylcellulose. Suspension culture was established by growing cells from the 3rd plating in RPMI with 10% FBS (Sigma) and 10ng/ul of mIL3 (Peprotech). To excise *Cbp in vitro,* cells with *Cbpfl/fl;*wt background from the 3rd plating were collected and transduced with pBabe-puro or pBabe-Cre-puro. Serial replating assays were set up as described above with 2ug/ml puromycin.

Mouse disease model. The *Cbp;*Mx1-Cre mouse model, transplantation procedures and tissue processing have been previously described[8,34]. To examine the requirement of *Cbp* for leukemia initiation, 1x10^6 *Cbp*-wt or *Cbp*-excised myeloid progenitor cells, which had been transduced with MSCV-MT2-IRES-GFP, were injected intravenously into lethally irradiated (2x550rads) C57BL/6 recipients. To examine the role of *Cbp* in the maintenance of leukemia, we first established MT2 induced AML by transplanting *Cbpfl/fl*;Mx$^+$ (with no pIpC treatment) cells that had been transduced with MSCV-MT2-IRES-GFP into lethally irradiated recipients. When mice demonstrated illness, spleen cells were collected and 10^6 cells were transplanted into sub-lethally irradiated (550rads) C57BL/6 recipients. To excise *Cbp in vivo*, 10 days after transplantation, 5 doses of pIpC were injected intraperitoneally. GFP$^+$ cells were sorted using a MoFlo Cell Sorter(Beckman Coulter). PCR primers for *Cbp* genotyping were: GGGGAAATTTTGGTCTGGTAAG(Forward), and CTGCTCTACCTAAATTCCCAG(Reverse). All mice were housed in a pathogen-free animal facility. Experiments were conducted under UK Home Office regulations.

RNAi experiments. p300 shRNA in pLKO.1 lentiviral vector and control vector targeting the Luciferase sequence(SHC007) were obtained from Sigma-Aldrich. Lentiviral supernatants were produced in 293T cells with packaging plasmids PSPAX2 and PMD2G (Sigma) using TransIT-LT1 reagent. Transduction of leukemia cell lines was performed using standard protocols[24] with puromycin (2ug/ml final concentration) as a selection marker. 10^4 transduced cells were plated in methylcellulose and suspension cultures were set up. To assess p300 expression, total mRNA was prepared using Trizol reagent (Invitrogen). cDNA was synthesized using SuperScript cDNA synthesis kit (Invitrogen). Quantitative RT-PCR was carried out with SYBR Green PCR mastermix using the ABI Prism 7000 system (Applied Biosystems). RNA expression levels were normalized to beta-actin.

Cell culture and methylcellulose assays. Kasumi-1, KG-1, ME-1, HEL, U937, SKM-1, Nomo-1, MOLM-13, OCI-AML3 and K562 cells were grown in RPMI-1640 medium (PAA) supplemented with FBS (10-20% final concentration, Sigma-Aldrich). Human CD34+ cells were maintained in liquid culture using StemSpan Serum-free media and CC100 cytokine cocktail (STEMCELL Technologies). All growth media also contained 1% penicillin/streptomycin. Unless otherwise stated, mouse BM, MT2 and NHA9 mouse immortalized progenitors, leukemic cell lines and human control $CD34^+$ and AML patient primary cells were plated at a concentration of 10,000-20,000 cells/plate (in duplicate) using the MethoCult™ H4531, MethoCult™ H4435 Enriched (for Human cells), or MethoCult™ GF M3434 (for mouse cells) (STEMCELL Technologies). Colonies were scored at 7-12 days.

p300/CBP KAT inhibitor (C646). Mouse and human cells were treated with the p300/CBP HAT inhibitor C646 (whose properties are described in detail in [25]), at various concentrations. The inactive form CM37 and DMSO vehicle were included as controls. For the liquid growth experiments, cells were re-suspended at a concentration of $0.5x10^6$ cells/ml, and the appropriate amount of drug was added. At the appropriate time points, wells were counted, washed in PBS and re-suspended at the same concentration, with fresh drug added each time.

Western blotting. Western blotting was performed using standard protocols (15% SDS-PAGE gels). Antibodies used: Histone 4 (17036,Abcam), Anti-acetyl-Histone H3 (06-599,Millipore). IRDye® 680RD and IRDye® 800CW were used as secondary antibodies (LI-COR). Immunoblots were scanned using an Odyssey® Infrared Imaging system.

Flow cytometry assays. The apoptosis assays were performed using the BD Pharmingen™ Apoptosis Detection kit. Cell cycle experiments were performed on 80% EtOH-fixed cells, using Propidium Iodide (Sigma-Aldrich). Flow cytometry was performed on a CyAn ADP FlowCytometer (Dako) or a BD LSRFortessa cell analyser and all data were analysed with FloJo software (Tree Star, Inc.).

Chromatin immunoprecipitation (ChIP) and ChIP-PCR assays. ChIP was performed on KG-1 cells harvested 24hours post-treatment as previously described[34]. IgG (I5006, Sigma) or H3K18Ac (ab1191, Abcam) antibodies were used (2.5mg/reaction). ChIP-PCR was carried out with SYBR Green PCR mastermix using the ABI Prism 7000 system (Applied Biosystems). The following primers were used: CCNE2:CCTTGCTTCCTCTCTTCTCCA(Forward)/GTGGTGGCGATCTTTCTTCC(Reverse), CDT1:TCGCTACGAGGATTGAGCG(Forward)/CCTGCAGCTGTCAAAGTAGG(Reverse), GMNN:TCGCTACGAGGATTGAGCG(Forward)/CCTGCAGCTGTCAAAGTAGG(Reverse), MCM3:GTGGACCGGATCTGTTTGG(Forward)/GGTGCCGGGAAGTTTAAGTC(Reverse), MCM5:GGTTCTTGTCTCCCCTGGTT(Forward)/CCGGACTCCAACCCCAGT(Reverse).

Patient material. Control $CD34^+$ human cells, patient BM or peripheral blood cells (>80% blasts) were obtained following donor/patient consent and under full ethical approval at each involved institute. Mutations were determined by solution capture hybridisation followed by deep sequencing with baits and mutation calling as defined in Papaemmanuil *et al.*[35].

Statistical analysis. Unless otherwise stated, all statistical analyses used Student's t-test on raw data. Values equal to, or less than 0.05 were considered statistically significant. Survival curves were constructed using the Kaplan-Meier method. Error bars represent SEM. Symbols: *, $P < 0.05$; **, $P < 0.01$; ***, $P < 0.0001$.

ENCODE mining, GEP and bioinformatic analysis. Illumina human whole genome 6 V2 gene expression data from all three cell lines were normalized using RMA algorithm and analysed in R[36]. P300 peaks for CREBBP in the K562 AML cell line were downloaded from the ENCODE project (http://genome.ucsc.edu/ENCODE/).

GSEA and leading edge analysis. GSEA analysis tools were obtained from http://www.broadinstitute.org/gsea/index.jsp. Default settings and all curated gene sets (c2.All.v3.0.symbols.gmt) were used for the analysis.

Acknowledgements. Funding in the Huntly laboratory comes from Cancer Research UK, Leukaemia Lymphoma Research, the Kay Kendal Leukaemia Fund, the Leukemia lymphoma Society of America, the Wellcome Trust, The Medical Research Council and an NIHR Cambridge Biomedical Research Centre grant. Patient samples were processed in the Cambridge Blood and Stem Cell Biobank.

Author contributions. BH, GG and W-IC designed the experiments, GG, W-IC, SJH, PG, AF and EP performed experiments. GG, WI-C, DR, EP, PC, BG and BH analysed data. CC, JMVD and PAC provided critical reagents. BH oversaw the study. BH, GG and W-IC wrote and all authors reviewed the manuscript.

Conflict of interest: The authors disclose no potential conflicts of interest.

References.

1. Estey E, Dohner H. Acute myeloid leukaemia. *Lancet*. 2006;368:1894-907.

2. Cancer Genome Atlas Research N. Genomic and epigenomic landscapes of adult de novo acute myeloid leukemia. *The New England journal of medicine*. 2013;368:2059-74.

3. Dawson MA, Kouzarides T, Huntly BJ. Targeting epigenetic readers in cancer. *The New England journal of medicine*. 2012;367:647-57.

4. Blobel GA. CREB-binding protein and p300: molecular integrators of hematopoietic transcription. *Blood*. 2000;95:745-55.

5. Gu W, Roeder RG. Activation of p53 sequence-specific DNA binding by acetylation of the p53 C-terminal domain. *Cell*. 1997;90:595-606.

6. Bedford DC, Kasper LH, Fukuyama T, Brindle PK. Target gene context influences the transcriptional requirement for the KAT3 family of CBP and p300 histone acetyltransferases. *Epigenetics*. 2010;5:9-15.

7. Rebel VI, Kung AL, Tanner EA, Yang H, Bronson RT, Livingston DM. Distinct roles for CREB-binding protein and p300 in hematopoietic stem cell self-renewal. *Proc Natl Acad Sci U S A*. 2002;99:14789-94.

8. Chan WI, Hannah RL, Dawson MA, Pridans C, Foster D, Joshi A*, et al.* The transcriptional coactivator Cbp regulates self-renewal and differentiation in adult hematopoietic stem cells. *Mol Cell Biol*. 2011;31:5046-60.

9. Pasqualucci L, Dominguez-Sola D, Chiarenza A, Fabbri G, Grunn A, Trifonov V*, et al.* Inactivating mutations of acetyltransferase genes in B-cell lymphoma. *Nature*.471:189-95.

10. Mullighan CG, Zhang J, Kasper LH, Lerach S, Payne-Turner D, Phillips LA*, et al.* CREBBP mutations in relapsed acute lymphoblastic leukaemia. *Nature*.471:235-9.

11. Holmfeldt L, Wei L, Diaz-Flores E, Walsh M, Zhang J, Ding L*, et al.* The genomic landscape of hypodiploid acute lymphoblastic leukemia. *Nature genetics*. 2013;45:242-52.

12. Roelfsema JH, Peters DJ. Rubinstein-Taybi syndrome: clinical and molecular overview. *Expert reviews in molecular medicine*. 2007;**9**:1-16.

13. Kung AL, Rebel VI, Bronson RT, Ch'ng LE, Sieff CA, Livingston DM*, et al.* Gene dose-dependent control of hematopoiesis and hematologic tumor suppression by CBP. *Genes & development*. 2000;**14**:272-7.

14. Taki T, Sako M, Tsuchida M, Hayashi Y. The t(11;16)(q23;p13) translocation in myelodysplastic syndrome fuses the MLL gene to the CBP gene. *Blood*. 1997;**89**:3945-50.

15. Ida K, Kitabayashi I, Taki T, Taniwaki M, Noro K, Yamamoto M*, et al.* Adenoviral E1A-associated protein p300 is involved in acute myeloid leukemia with t(11;22)(q23;q13). *Blood*. 1997;**90**:4699-704.

16. Deguchi K, Ayton P, Carapeti M, Kutok J, Snyder C, Williams I*, et al.* MOZ-TIF2-induced acute myeloid leukemia requires the MOZ nucleosome binding motif and TIF2-mediated recruitment of CBP. *Cancer Cell*. 2003;**3**:259-71.

17. Kasper LH, Brindle PK, Schnabel CA, Pritchard CE, Cleary ML, van Deursen JM. CREB binding protein interacts with nucleoporin-specific FG repeats that activate transcription and mediate NUP98-HOXA9 oncogenicity. *Mol Cell Biol*. 1999;**19**:764-76.

18. So CW, Cleary ML. MLL-AFX requires the transcriptional effector domains of AFX to transform myeloid progenitors and transdominantly interfere with forkhead protein function. *Mol Cell Biol*. 2002;**22**:6542-52.

19. Bayly R, Chuen L, Currie RA, Hyndman BD, Casselman R, Blobel GA*, et al.* E2A-PBX1 interacts directly with the KIX domain of CBP/p300 in the induction of proliferation in primary hematopoietic cells. *J Biol Chem*. 2004;**279**:55362-71.

20. Payne SR, Kemp CJ. Tumor suppressor genetics. *Carcinogenesis*. 2005;**26**:2031-45.

21. Jemal A, Siegel R, Ward E, Hao Y, Xu J, Murray T*, et al.* Cancer statistics, 2008. *CA Cancer J Clin*. 2008;**58**:71-96.

22. Oki Y, Issa JP. Epigenetic mechanisms in AML - a target for therapy. *Cancer Treat Res*. 2010;**145**:19-40.

23. Baljevic M, Park JH, Stein E, Douer D, Altman JK, Tallman MS. Curing all patients with acute promyelocytic leukemia: are we there yet? *Hematology/oncology clinics of North America*. 2011;**25**:1215-33, viii.

24. Huntly BJ, Shigematsu H, Deguchi K, Lee BH, Mizuno S, Duclos N*, et al.* MOZ-TIF2, but not BCR-ABL, confers properties of leukemic stem cells to committed murine hematopoietic progenitors. *Cancer Cell*. 2004;**6**:587-96.

25. Bowers EM, Yan G, Mukherjee C, Orry A, Wang L, Holbert MA*, et al.* Virtual ligand screening of the p300/CBP histone acetyltransferase: identification of a selective small molecule inhibitor. *Chem Biol*. 2010;**17**:471-82.

26. Consortium EP. A user's guide to the encyclopedia of DNA elements (ENCODE). *PLoS biology*. 2011;**9**:e1001046.

27. Walter RB, Appelbaum FR, Estey EH, Bernstein ID. Acute myeloid leukemia stem cells and CD33-targeted immunotherapy. *Blood*. 2012;**119**:6198-208.

28. Grunwald MR, Levis MJ. FLT3 inhibitors for acute myeloid leukemia: a review of their efficacy and mechanisms of resistance. *International journal of hematology*. 2013;**97**:683-94.

29. Kimbrel EA, Lemieux ME, Xia X, Davis TN, Rebel VI, Kung AL. Systematic in vivo structure-function analysis of p300 in hematopoiesis. *Blood*. 2009;**114**:4804-12.

30. Allard S, Masson JY, Cote J. Chromatin remodeling and the maintenance of genome integrity. *Biochimica et biophysica acta*. 2004;**1677**:158-64.

31. Gang EJ, Hsieh YT, Pham J, Zhao Y, Nguyen C, Huantes S*, et al.* Small-molecule inhibition of CBP/catenin interactions eliminates drug-resistant clones in acute lymphoblastic leukemia. *Oncogene*. 2013.

32. Wang L, Gural A, Sun XJ, Zhao X, Perna F, Huang G*, et al.* The leukemogenicity of AML1-ETO is dependent on site-specific lysine acetylation. *Science*. 2011;**333**:765-9.

33. Gao XN, Lin J, Ning QY, Gao L, Yao YS, Zhou JH*, et al.* A histone acetyltransferase p300 inhibitor C646 induces cell cycle arrest and apoptosis selectively in AML1-ETO-positive AML cells. *PloS one*. 2013;**8**:e55481.

34. Dawson MA, Prinjha RK, Dittmann A, Giotopoulos G, Bantscheff M, Chan WI*, et al.* Inhibition of BET recruitment to chromatin as an effective treatment for MLL-fusion leukaemia. *Nature*. 2011;**478**:529-33.

35. Papaemmanuil E, Gerstung M, Malcovati L, Tauro S, Gundem G, Van Loo P*, et al.* Clinical and biological implications of driver mutations in myelodysplastic syndromes. *Blood*. 2013.

36. Ihaka R, Gentleman R. R:A language for data analysis and graphics. *Journal of Computational and Graphical Statistics*. 1996;**5**:299-314.

Figure legends.

Figure 1: *Cbp*$^{-/-}$ cells are rapidly outcompeted by *Cbp* wt cells, under selective *in vitro* conditions, in MT2- and NHA9-driven AML.

A. Serial replating assays of MT2- and NHA9-driven leukemias demonstrate no difference in colony number or serial replating activity between transduced *Cbp* wt and *Cbp*$^{-/-}$ progenitor cells. B. Similar replating assays demonstrate no differences in the *in vitro* self-renewal potential of MT2 and NHA9 AML murine cell lines generated from *Cbpfl/fl* progenitors following expression of either Cre-puro or an empty puro vector, as both cell lines retained serial replating potential post-*Cbp* excision. C. Genotyping of pooled colonies at the end of each round of replating, revealed serial re-emergence of the un-excised *Cbp* allele, in the NHA9 and MT2, but not in the ME immortalized murine cell lines.

Figure 2: *Cbp* confers a selective advantage during initiation/progression of MT2-driven AML, under selective *in vivo* conditions.

A. *Cbp* wt and *Cbp*$^{-/-}$ progenitor cells were transduced with MT2 and transplanted into lethally irradiated recipients. Genotyping of the *Cbp* wt and *Cbp*$^{-/-}$ progenitor cells post-transduction confirmed almost complete excision of the *Cbp* allele. However, genotyping of leukemic cells revealed re-emergence and clonal expansion of the un-excised *Cbp* allele. Furthermore, enrichment of leukemic cells via GFP sorting demonstrated only non-recombined cells, suggesting that Cbp loss confers a significant growth disadvantage during leukemia induction. All recipient mice succumbed to AML within 4 months post-transplantation. B. c-kit^{+} *Cbpfl/fl;*Mx1-Cre^{+} BM cells were transduced with MT2 and transplanted into lethally irradiated recipients. The leukemias that arose in the primary recipients were transplanted into secondary animals. Excision of the *Cbp* allele in the secondary recipient animals resulted in decreased penetration of disease (only 40% of animals developed AML). Representative flow cytometry demonstrates that no GFP^{+} cells could be detected in the peripheral blood of non-diseased animals at the end of the experiment (d120).

Figure 3: Functional redundancy of Cbp and p300 during myeloid transformation.

A. *p300* expression following lentiviral transduction of *Cbp*$^{-/-}$ cells, using two different shRNAs. Expression was assessed by q-PCR using beta-actin as a reference gene. B. sh-mediated knockdown of p300 decreases clonogenic potential of MT2 and NHA9 AML cell lines, particularly on a *Cbp*$^{-/-}$ background.

Figure 4: Pharmacological inhibition of CBP and P300, suppresses the growth and decreases clonogenic potential of multiple AML cell lines *in vitro*.

A. C646 treatment of normal murine BM cells (n=3) does not lead to significant changes of the number, or the types of colonies produced in serial replating assays. B. C646 suppresses the growth of the NHA9 immortalized murine cell line in liquid culture and in methylcellulose assays. C. Ten different human AML cell lines were tested against C646, over a period of 12 days in liquid culture conditions. The majority of these were responsive to C646 treatment (e.g. Kasumi-1), with 7/10 cell lines demonstrating a >50% decrease in cell numbers on day 12, compared to DMSO control. Two cell lines showed no response to CBP/p300 KAT inhibition (K562 and MOLM13). D. Similarly, methylcellulose assays revealed a significant decrease in clonogenic potential in 8/10 human AML cell lines treated with C646. E. Treatment with C646 induces apoptosis in the sensitive (Kasumi-1) but not the resistant (K562) cell lines, as measured by Annexin/7-AAD staining. F. Induction of apoptosis in the sensitive cell lines is accompanied by a modest G1 cell cycle arrest (assessed by PI staining), however this is lacking in the resistant K562 cell line.

Figure 5: C646 treatment results in distinct transcriptional and chromatin acetylation changes associated with genomic integrity in sensitive AML cell lines.

A. Volcano plots for C646 *vs.* DMSO treated samples (KG-1, Kasumi-1 and K562), showing fold-change (log_2) and *p*-value significance level (log_{10}) for all genes. A larger number of genes are differentially

regulated in the sensitive (KG1 and Kasumi-1) versus the resistant (K562) cell line. **B.** Log fold change correlation plot for all genes between the sensitive KG-1 and Kasumi-1 following treatment, demonstrating a high degree of similarity in the transcriptional changes induced by C646. **C.** Venn diagram of genes significantly differentially regulated (1.5 FC; <0.05 adj. *p*-value) upon C646 treatment, between the different cell lines (left panel). Heatmap for the common list of genes (87 genes) found to be deregulated upon treatment in KG-1 and Kasumi-1 but not in K562 cells (right panel). **E.** The "common" gene list was subjected to a Gene Ontology (Molecular Function) over-representation analysis. The significant results were displayed using a heatmap to highlight the percentage of shared gene between the categories, and demonstrates enrichment for processes including cell cycle control, mitosis and DNA replication and repair. **E.** ChIP-PCR analysis of H3K18 acetylation levels (24hours post-treatment) in the promoter regions of selected candidates from the list of the 87 downregulated genes.

Figure 6: C646 treatment decreases growth of primary human AML samples.

A. C646 treatment of normal human CD43+cells (n=2) did not alter their clonogenic potential. **B.** No induction of apoptosis was observed following treatment of normal CD34+ cells with C646, as measured by Annexin/7-AAD staining. **C.** By contrast, a significant reduction in colony numbers was seen in 19/29 primary AML samples exposed to the C646 compound. **D.** A number of primary AML samples (n=29), covering a range of molecular subtypes, with variable karyotypic mutational and prognostic status, as shown in this table were assessed for sensitivity to C646 (see text and Supplementary Figure 6).

Figure 1

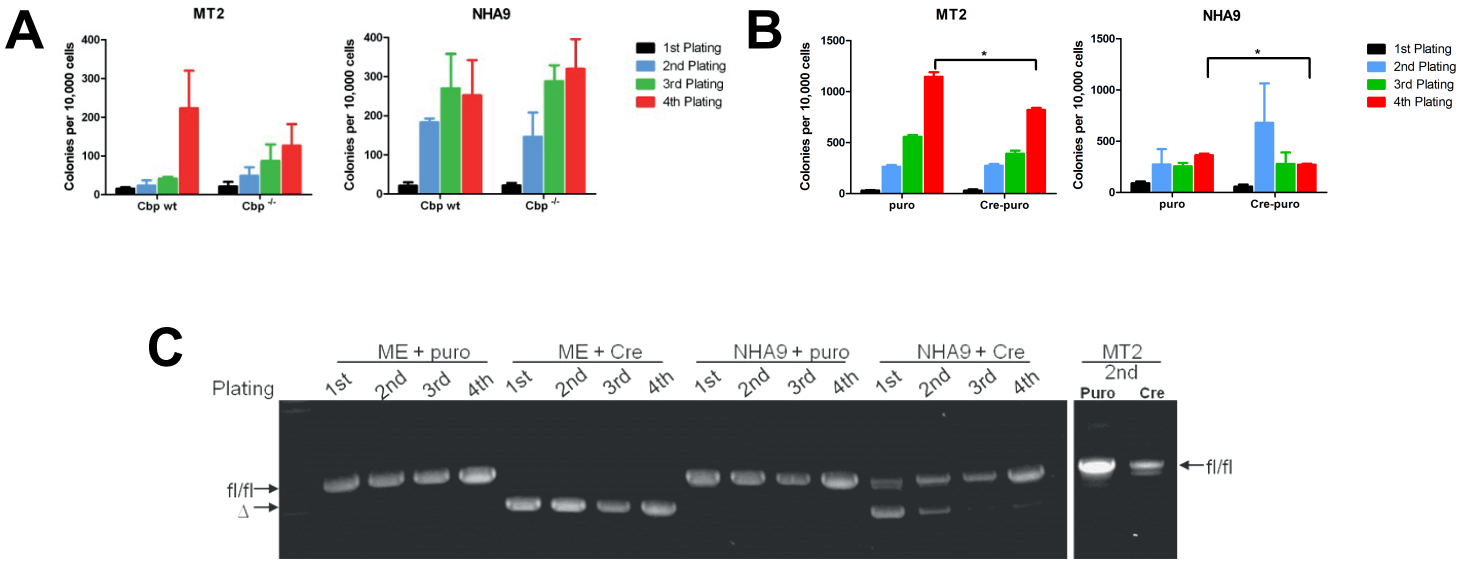
A
MT2
NHA9
Colonies per 10,000 cells
Cbp wt
Cbp -/-
1st Plating
2nd Plating
3rd Plating
4th Plating
B
MT2
NHA9
puro
Cre-puro
*
C
Plating
ME + puro
ME + Cre
NHA9 + puro
NHA9 + Cre
MT2
2nd
Puro
Cre
1st
2nd
3rd
4th
fl/fl
Δ

Figure 2

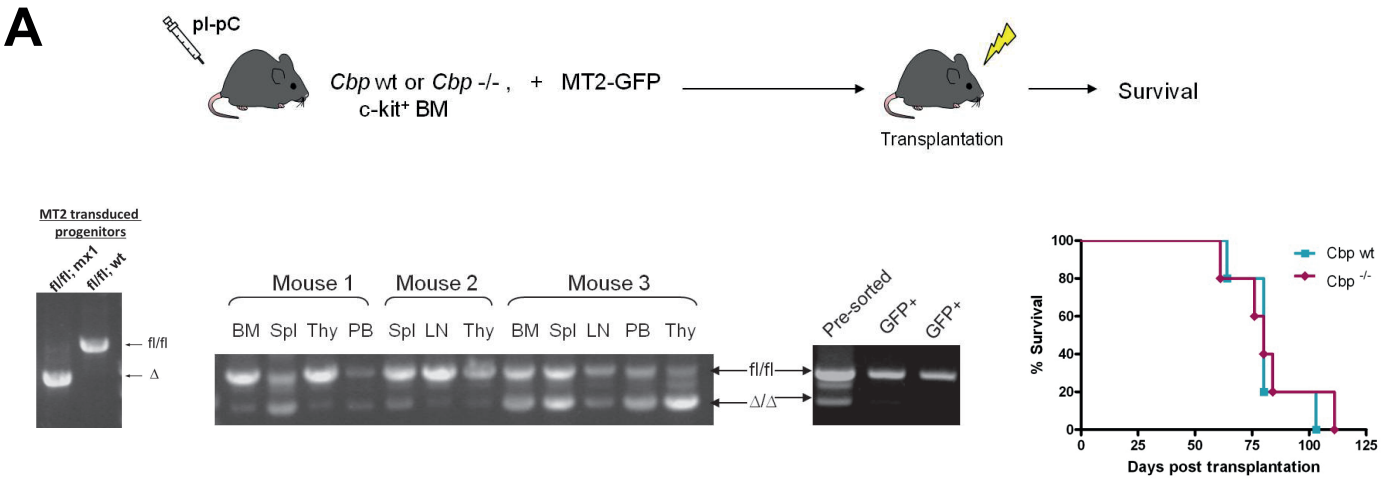
A
pI-pC
Cbp wt or Cbp -/- ,
c-kit+ BM
+ MT2-GFP
Transplantation
Survival
MT2 transduced progenitors
fl/fl; mx1
fl/fl; wt
fl/fl
Δ
Mouse 1
Mouse 2
Mouse 3
BM Spl Thy PB Spl LN Thy BM Spl LN PB Thy
Pre-sorted
GFP+
GFP+
fl/fl
Δ/Δ
% Survival
Days post transplantation
Cbp wt
Cbp -/-

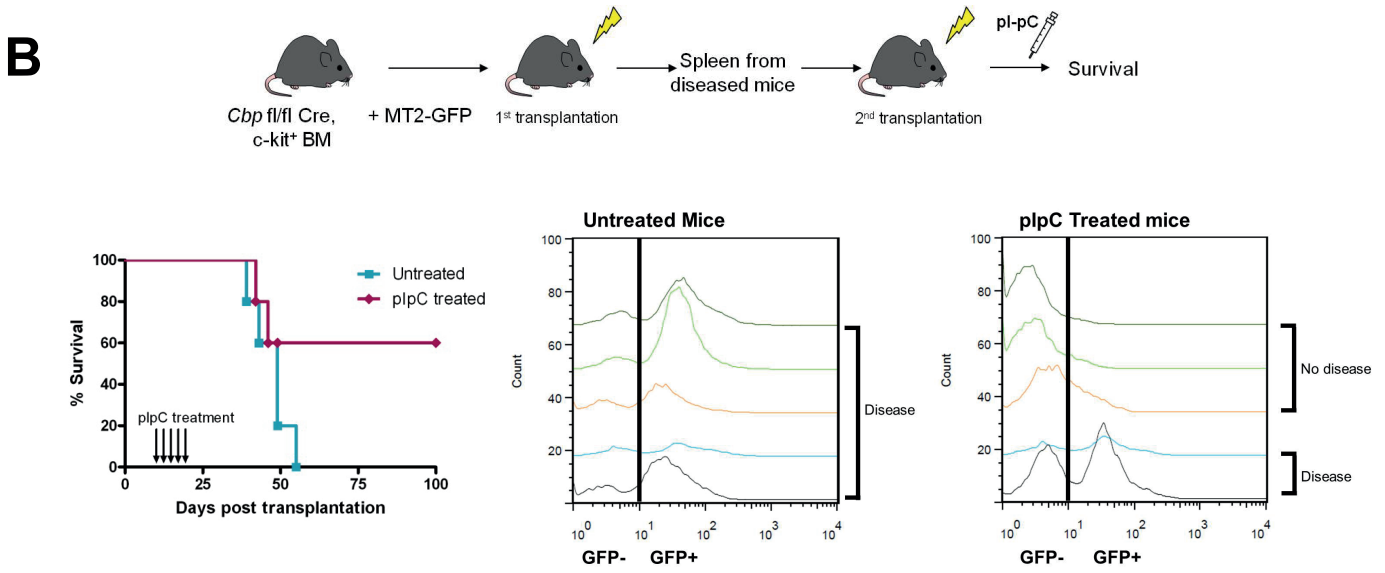
B
Cbp fl/fl Cre,
c-kit+ BM
+ MT2-GFP
1st transplantation
Spleen from diseased mice
2nd transplantation
pI-pC
Survival
% Survival
Untreated
pIpC treated
pIpC treatment
Days post transplantation
Untreated Mice
pIpC Treated mice
Count
Disease
No disease
GFP-
GFP+

Figure 3

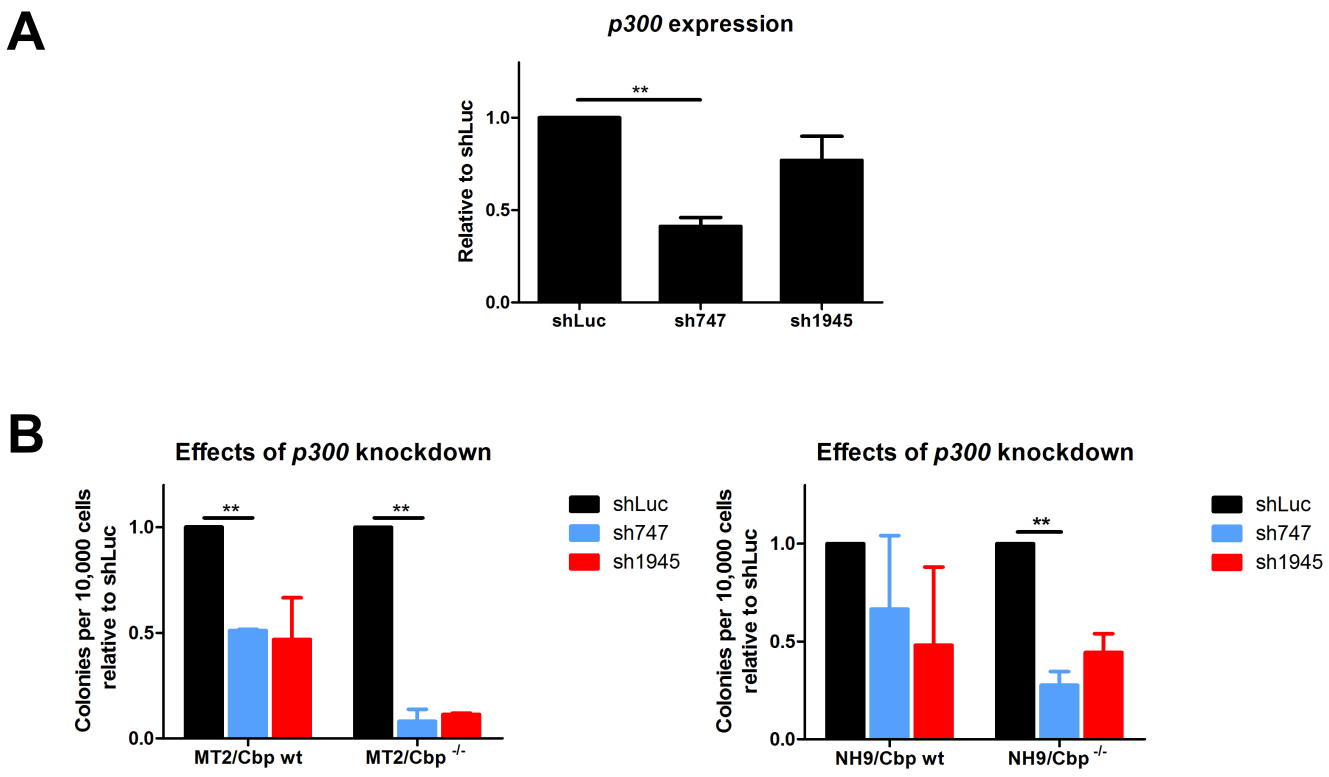
A
p300 expression
Relative to shLuc
1.0
0.5
0.0
**
shLuc
sh747
sh1945
B
Effects of p300 knockdown
Colonies per 10,000 cells relative to shLuc
1.0
0.5
0.0
**
**
MT2/Cbp wt
MT2/Cbp -/-
shLuc
sh747
sh1945
Effects of p300 knockdown
Colonies per 10,000 cells relative to shLuc
1.0
0.5
0.0
**
NH9/Cbp wt
NH9/Cbp -/-
shLuc
sh747
sh1945

Figure 4

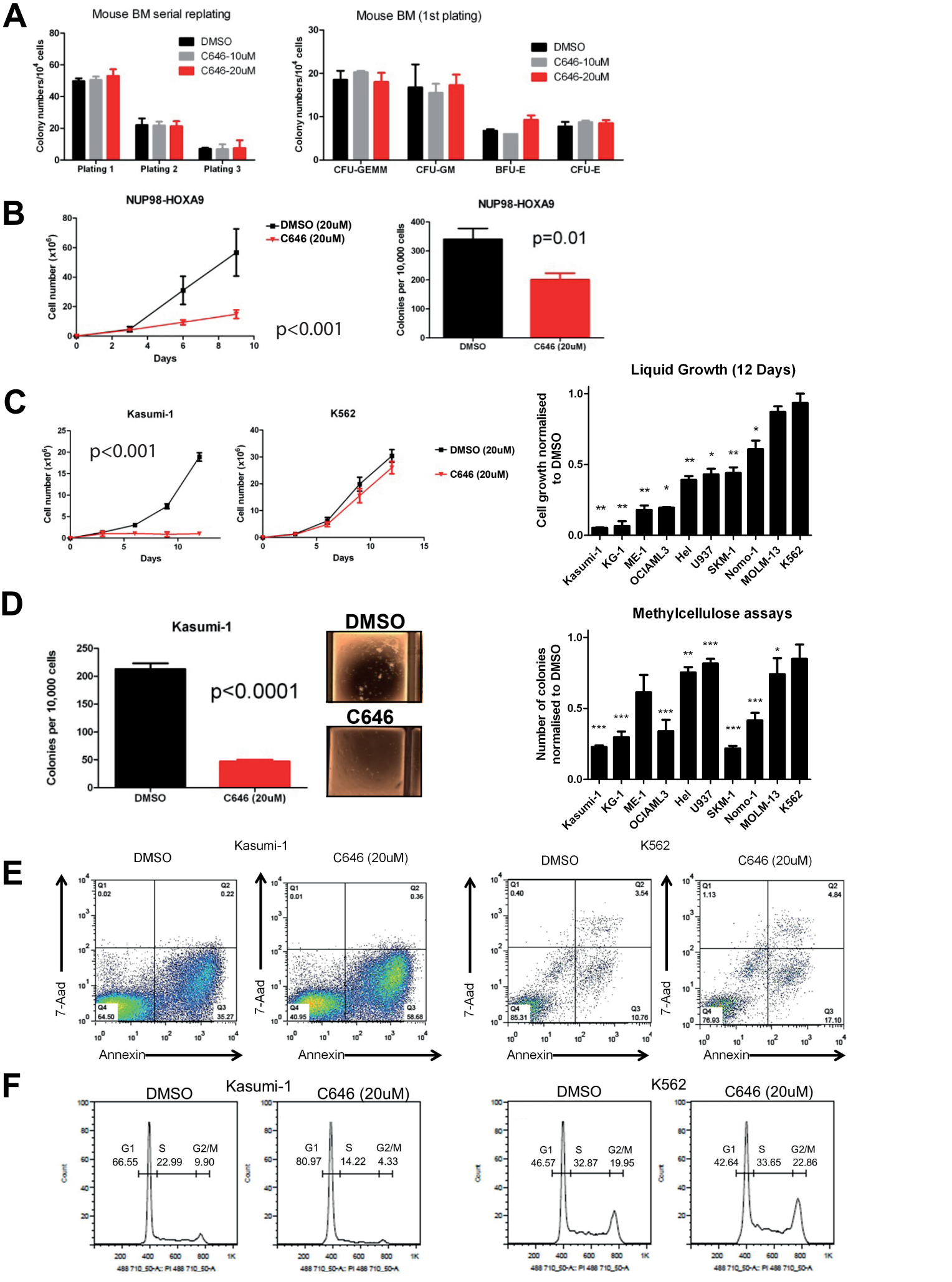
A
Mouse BM serial replating
Colony numbers/10^4 cells
DMSO
C646-10uM
C646-20uM
Plating 1
Plating 2
Plating 3
Mouse BM (1st plating)
CFU-GEMM
CFU-GM
BFU-E
CFU-E
B
NUP98-HOXA9
Cell number (x10^6)
DMSO (20uM)
C646 (20uM)
Days
p<0.001
NUP98-HOXA9
Colonies per 10,000 cells
p=0.01
C
Kasumi-1
K562
p<0.001
Liquid Growth (12 Days)
Cell growth normalised to DMSO
Kasumi-1
KG-1
ME-1
OCIAML3
Hel
U937
SKM-1
Nomo-1
MOLM-13
K562
D
Kasumi-1
Colonies per 10,000 cells
p<0.0001
DMSO
C646
C646 (20uM)
Methylcellulose assays
Number of colonies normalised to DMSO
E
Kasumi-1
K562
DMSO
C646 (20uM)
7-Aad
Annexin
F
DMSO
C646 (20uM)
G1
S
G2/M
66.55
22.99
9.90
80.97
14.22
4.33
46.57
32.87
19.95
42.64
33.65
22.86

Figure 5

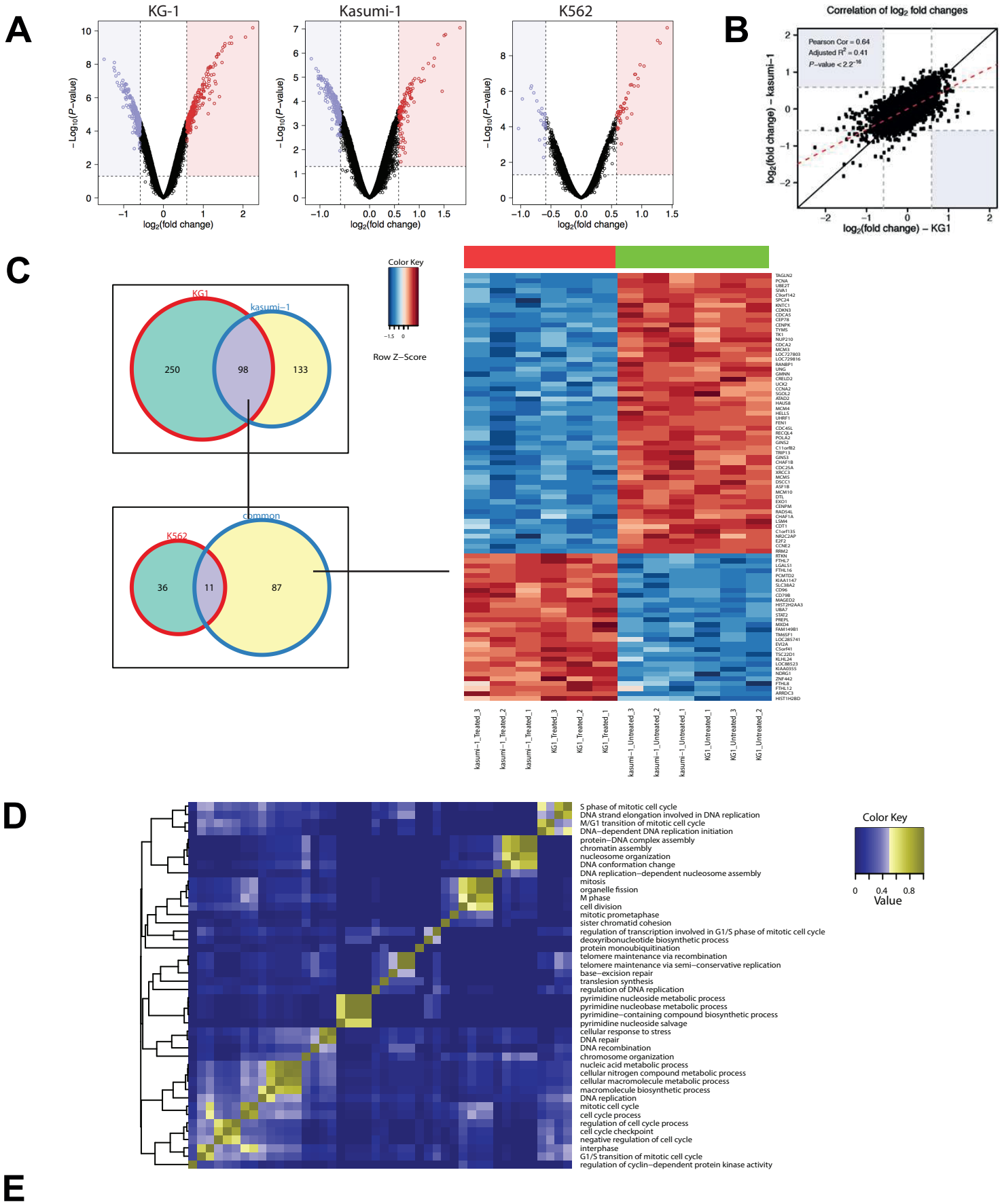
A
KG-1
Kasumi-1
K562
−Log10(P−value)
log2(fold change)
B
Correlation of log2 fold changes
Pearson Cor = 0.64
Adjusted R2 = 0.41
P−value < 2.2−16
log2(fold change) − kasumi−1
log2(fold change) − KG1
C
KG1
kasumi−1
250
98
133
common
K562
36
11
87
Color Key
Row Z−Score
kasumi−1_Treated_3
kasumi−1_Treated_2
kasumi−1_Treated_1
KG1_Treated_3
KG1_Treated_2
KG1_Treated_1
kasumi−1_Untreated_3
kasumi−1_Untreated_2
kasumi−1_Untreated_1
KG1_Untreated_1
KG1_Untreated_3
KG1_Untreated_2
D
S phase of mitotic cell cycle
DNA strand elongation involved in DNA replication
M/G1 transition of mitotic cell cycle
DNA−dependent DNA replication initiation
protein−DNA complex assembly
chromatin assembly
nucleosome organization
DNA conformation change
DNA replication−dependent nucleosome assembly
mitosis
organelle fission
M phase
cell division
mitotic prometaphase
sister chromatid cohesion
regulation of transcription involved in G1/S phase of mitotic cell cycle
deoxyribonucleotide biosynthetic process
protein monoubiquitination
telomere maintenance via recombination
telomere maintenance via semi−conservative replication
base−excision repair
translesion synthesis
regulation of DNA replication
pyrimidine nucleoside metabolic process
pyrimidine nucleobase metabolic process
pyrimidine−containing compound biosynthetic process
pyrimidine nucleoside salvage
cellular response to stress
DNA repair
DNA recombination
chromosome organization
nucleic acid metabolic process
cellular nitrogen compound metabolic process
cellular macromolecule metabolic process
macromolecule biosynthetic process
DNA replication
mitotic cell cycle
cell cycle process
regulation of cell cycle process
cell cycle checkpoint
negative regulation of cell cycle
interphase
G1/S transition of mitotic cell cycle
regulation of cyclin−dependent protein kinase activity
Color Key
Value
E
CCNE2
CDT1
GMNN
MCM3
MCM5
% Input
DMSO IgG
646 IgG
DMSO H3K18Ac
646 H3K18Ac

Figure 6

A

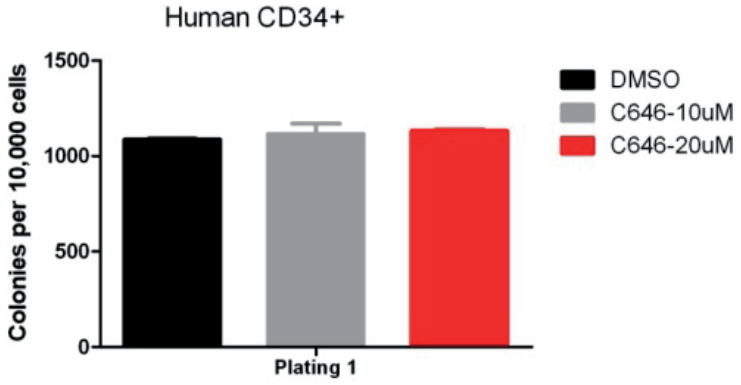

B

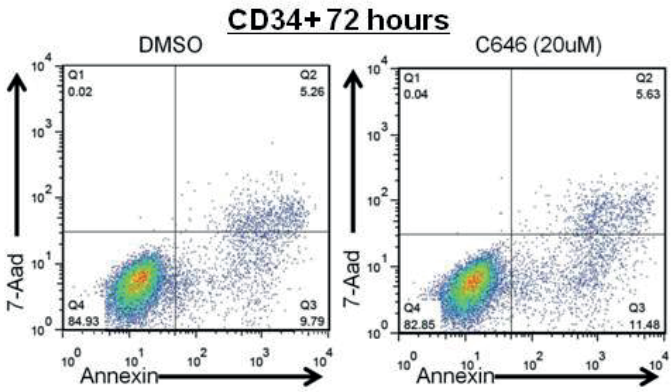

C

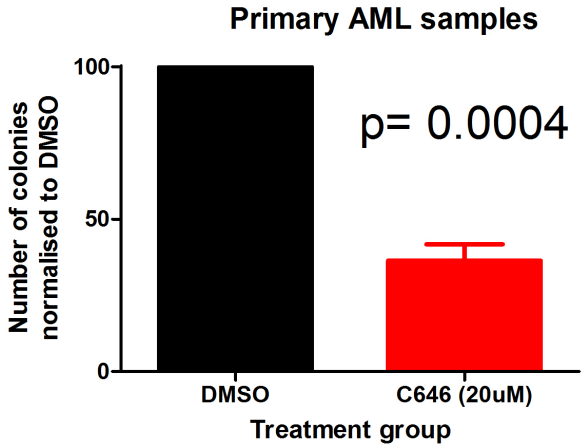

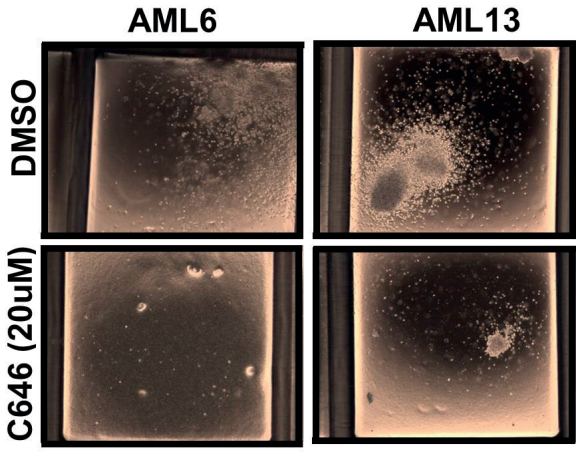

D

Patient	Sex	Age	Karyotype	NPM1 status	FLT3 Status	Other mutations*
AML 1	F	79	46 XX, i17(q)	WT	WT	MPL, TET2, U2AF1
AML 2	F	68	46 XX Add 11(p15)	NPM1c	TKD	TET2, DNMT3A
AML 3	M	47	46 XY	NPM1c	TKD	DNMT3A, IDH1, CUX1, PTPN11
AML 4	M	64	46 XY	NPM1c	WT	KRAS, KDM2B
AML 5	M	50	46 XY, t(15;17)	WT	ITD	WT1, ASXL1, FAM175B
AML 6	M	24	46 XY, inv(16)	WT	TKD	NRAS
AML 7	F	70	ND	WT	WT	ND
AML 8	M	78	46 XY, 3q(26)	WT	ITD	DNMT3A, U2AF1, CTNNA1
AML 9	M	50	46 XY, t(15;17)	WT	ITD	NONE
AML 10	M	55	46 XY, t(3;7)	WT	TKD	TP53, SFRS2, ASXL1
AML 11	F	63	Failed	WT	ITD	DNMT3A, TET2, CREBBP
AML 12	M	70	46 XY	WT	WT	TET2, PHF6, KRAS, FOSB
AML 13	M	82	Failed	WT	WT	ND
AML 14	F	44	46 XX, +15	WT	WT	ND
AML 15	F	28	46 XX, t(8;21)	WT	WT	ND

Patient	Sex	Age	Karyotype	NPM1 status	FLT3 Status	Other mutations*
AML 16	M	67	Failed	WT	WT	ND
AML 17	F	55	46 XX	NPM1c	WT	ND
AML 18	F	53	46 XX	WT	WT	ND
AML 19	M	44	46 XY	WT	WT	ND
AML 20	M	20	46 XY, Add 8(p21), MLL translocation	WT	WT	ND
AML 21	F	58	Complex (+6,add(10),t(11;19),+13,+ider(19),+21)	WT	WT	ND
AML 22	M	63	46 XY, t(15;17), +8	WT	WT	ND
AML 23	F	55	Complex (-5q, -7q, -10q, -12p, -16, +11)	WT	WT	ND
AML 24	M	38	46 XY	NPM1c	WT	ND
AML 25	F	65	46 XX	NPM1c	WT	ND
AML 26	F	71	46 XX	WT	WT	ND
AML 27	M	19	46 XY	NPM1c	ITD	ND
AML 28	M	74	46 XY	WT	ITD	ND
AML 29	M	71	ND	ND	ND	ND

Files in this Data Supplement (brief description):

Supplementary Figure 1: Recipients of MT2-transduced *Cbp* wt and *Cbp*$^{-/-}$ BM progenitor cells developed an AML of similar macroscopic and histological phenotype.

Supplementary Figure 2: Treatment with C646, but not its inactive analogue C37, results in induction of apoptosis and a marked decrease of H3 acetylation levels.

Supplementary Figure 3: Treatment with C646 demonstrates efficacy across multiple, but not all, AML subtypes.

Supplementary Figure 4: Time-frame of C646 apoptosis induction.

Supplementary Figure 5: Representative GSEA plots from gene expression profiles of C646-sensitive cell lines.

Supplementary Figure 6: Additional patient details for all primary AML samples used in methylcellulose assays.

Supplementary Table 1: Mutations reported in the human AML cell lines used in this study.

Supplementary Table 2: List of genes significantly deregulated in sensitive cell lines following treatment with C646.

Supplementary Figure legends

Supplementary Figure 1: MT2 transduced *Cbp* wt and *Cbp*$^{-/-}$ progenitor cells were transplanted into lethally irradiated recipient mice. All mice developed AML. Histology sections of BM (400x magnification), spleen (4x and 400x magnification), liver (4x and 400x magnification) and kidney (4x and 400x magnification), as well as weights of spleen and liver, at the experimental endpoint, reveal a similar phenotype between the two groups.

Supplementary Figure 2: A. Inhibition of KAT activity results in a marked decrease of histone 3 acetylation (H3Ac) levels in multiple human AML cell lines **B.** Treatment of Kasumi-1 cells with C37 (an inactive enantiomer of C646) had no impact on cellular viability, compared to DMSO and C646 conditions.

Supplementary Figure 3: A. Treatment of MT2 immortalized murine cells with C646, significantly reduced their cell growth (12 days in liquid culture) and, to a lesser extent, their colony numbers (methylcellulose assays). **B.** Treatment of the resistant cell line K562 with C646 had no impact on its clonogenic potential (assessed by methylcellulose assays). **C.** Treatment of human AML cell lines with C646, resulted in decreased viability (assessed by Annexin/7-AAD staining), relative to DMSO treatment.

Supplementary Figure 4: Treatment of the C646 sensitive cell lines demonstrates induction of apoptosis from 48 hours onwards, with no effect apparent at 24 hours.

Supplementary Figure 5: Representative GSEA plots demonstrating that treatment with C646 affects DNA replication and cell cycle progression pathways in both sensitive cell lines.

Supplementary Figure 6: Nineteen responder (black columns, >50% reduction in colony numbers when treated with C646) *vs.* 10 non-responder (grey columns, <50% reduction in colony numbers when treated with C646) primary AML samples following *in vitro* treatment in methylcellulose assays. Table: Additional prognosis information on patient used in this study.

Supplementary Table 1: Mutations in human AML cell lines.

Supplementary Table 2: Genes differentially expressed following treatment with C646.

Supplementary Figure 1

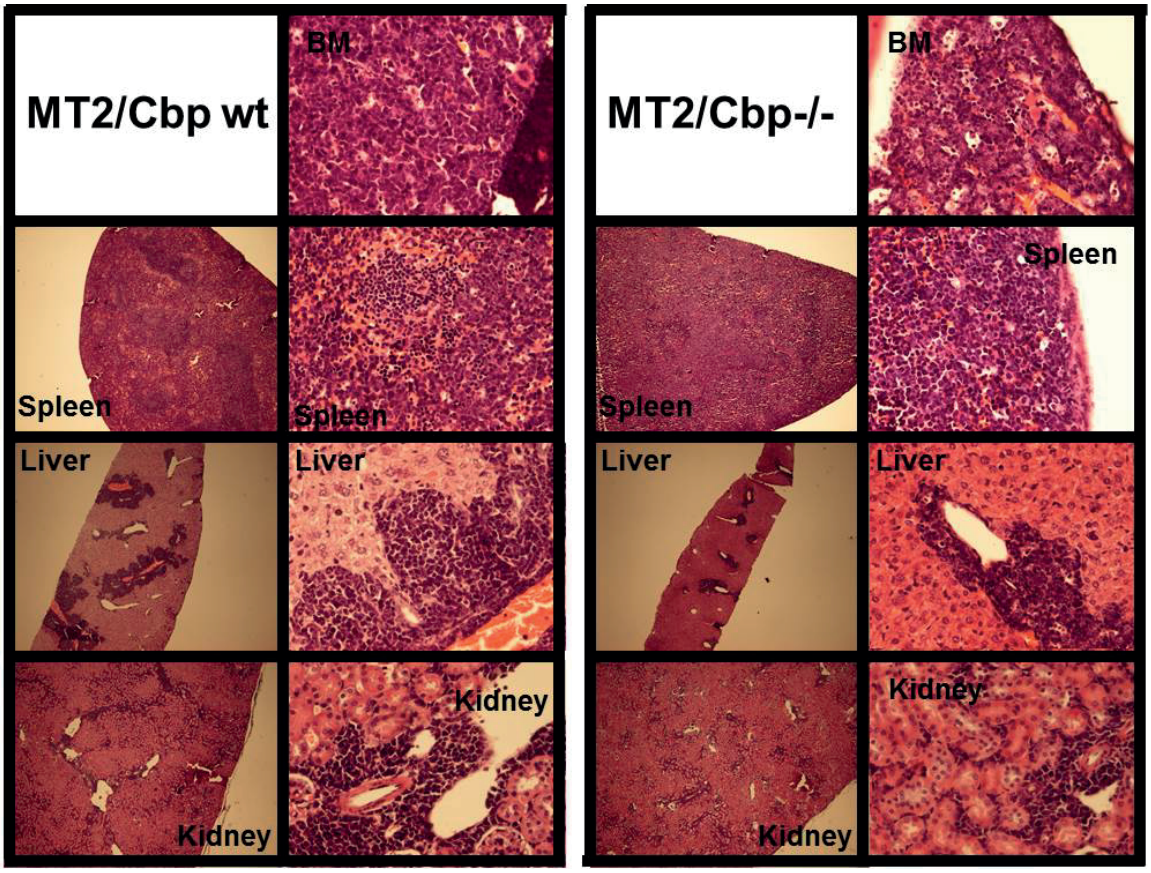

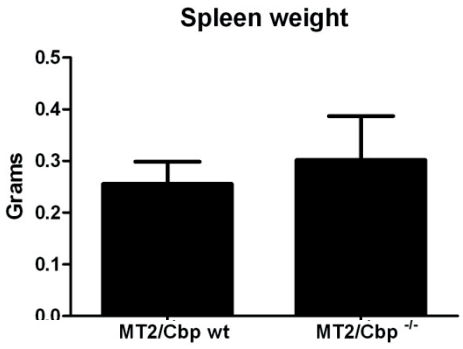

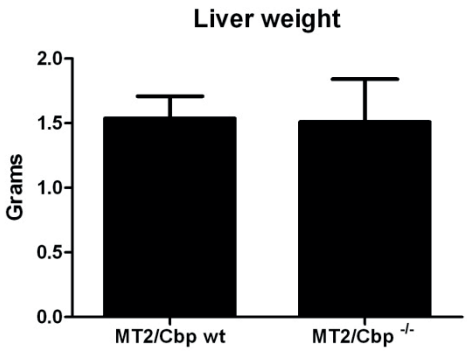

Supplementary Figure 2

A

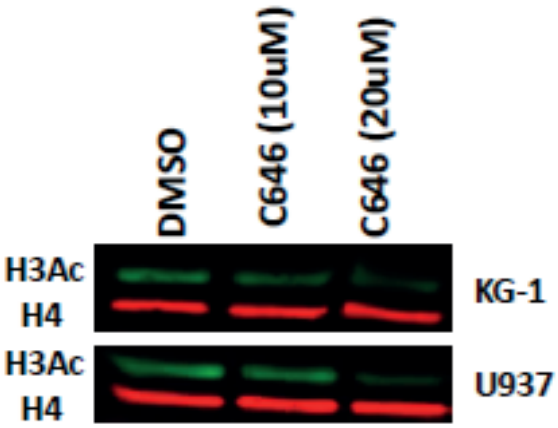

B

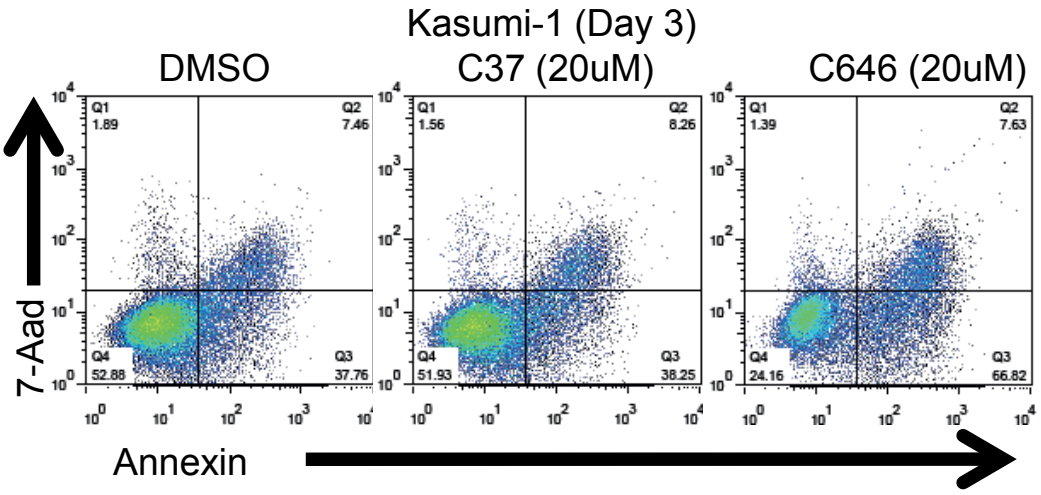

Supplementary Figure 3

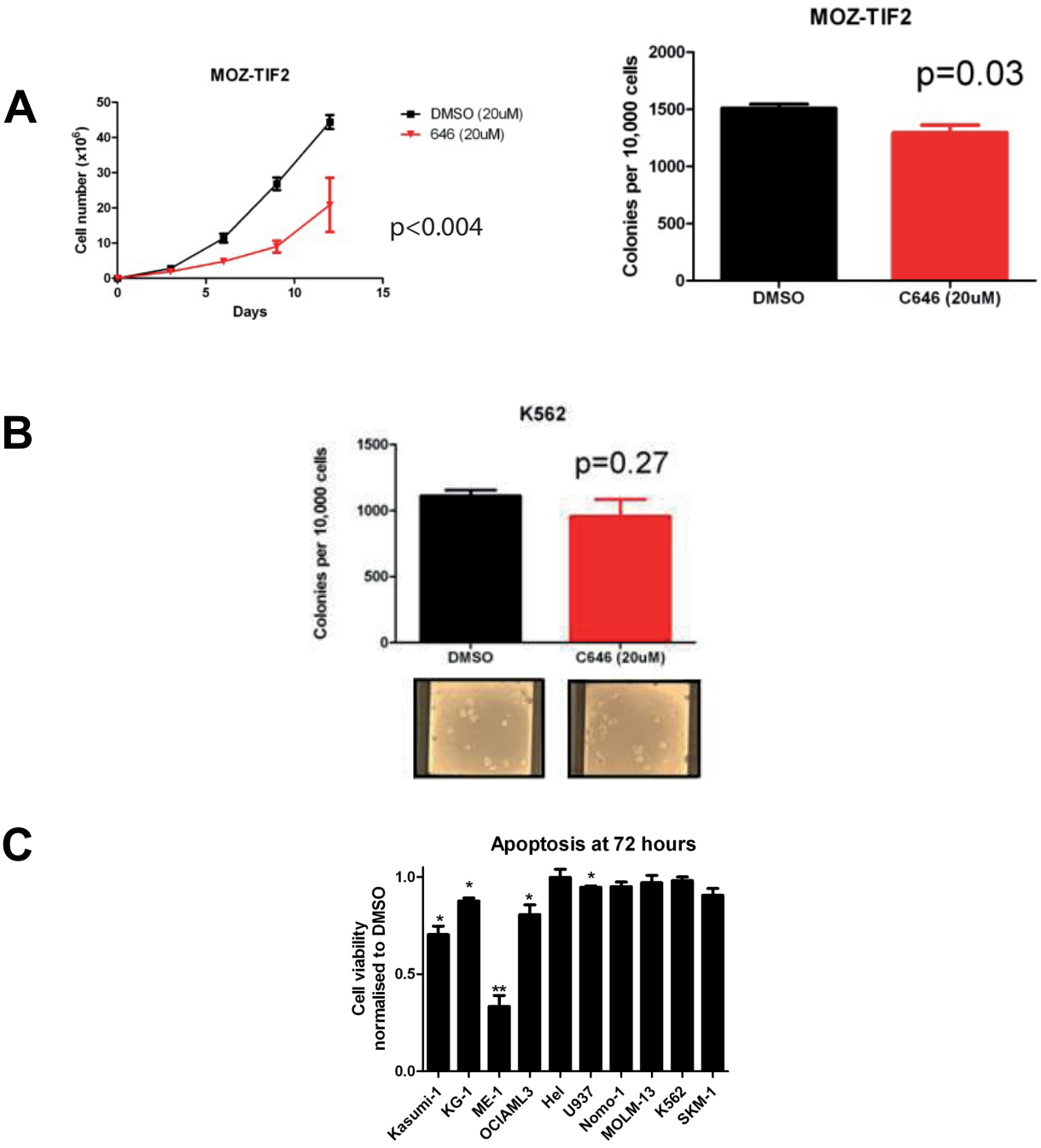

Supplementary Figure 4

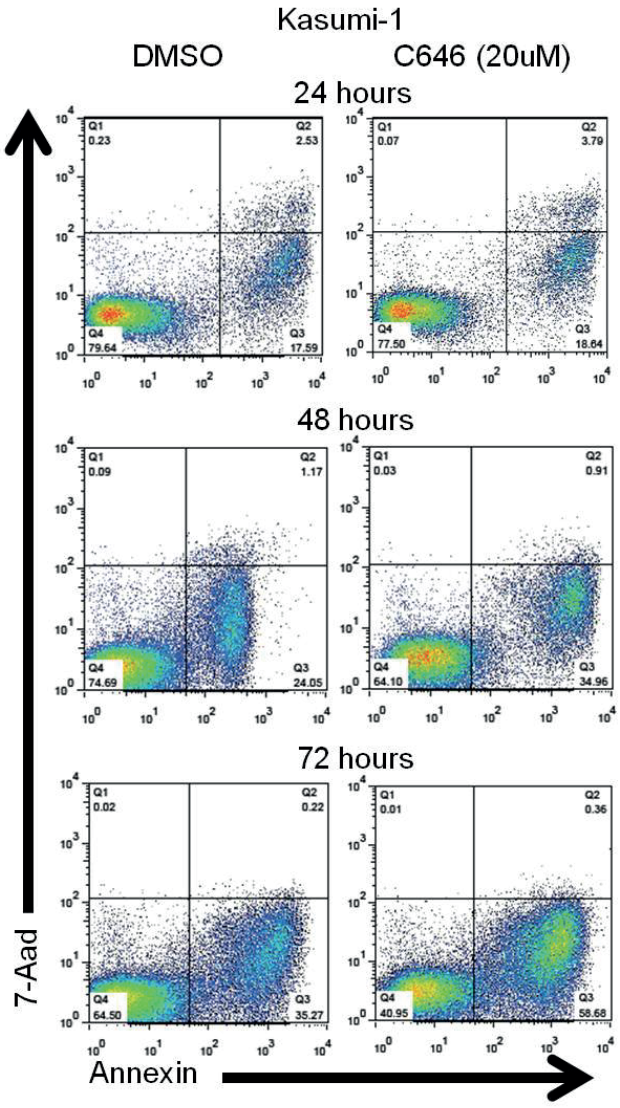

Supplementary Figure 5

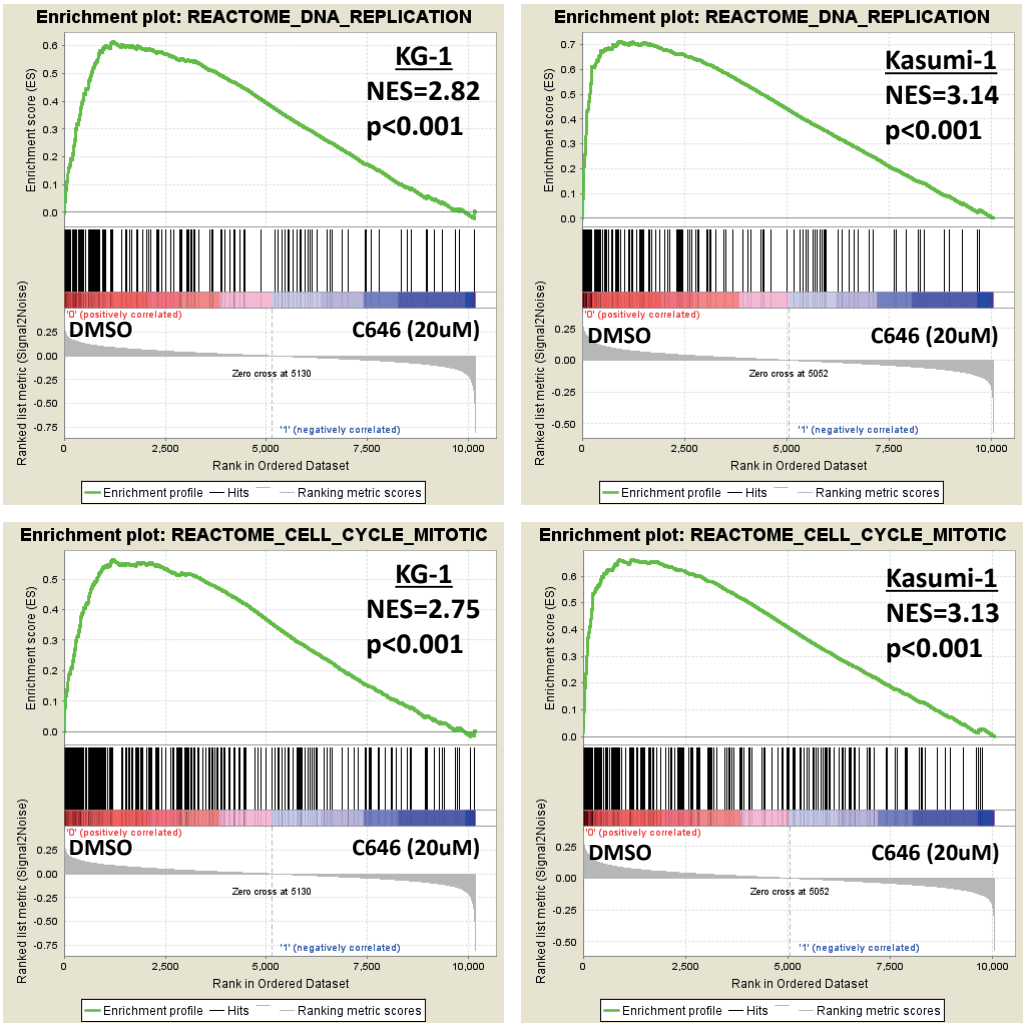

Supplementary Figure 6

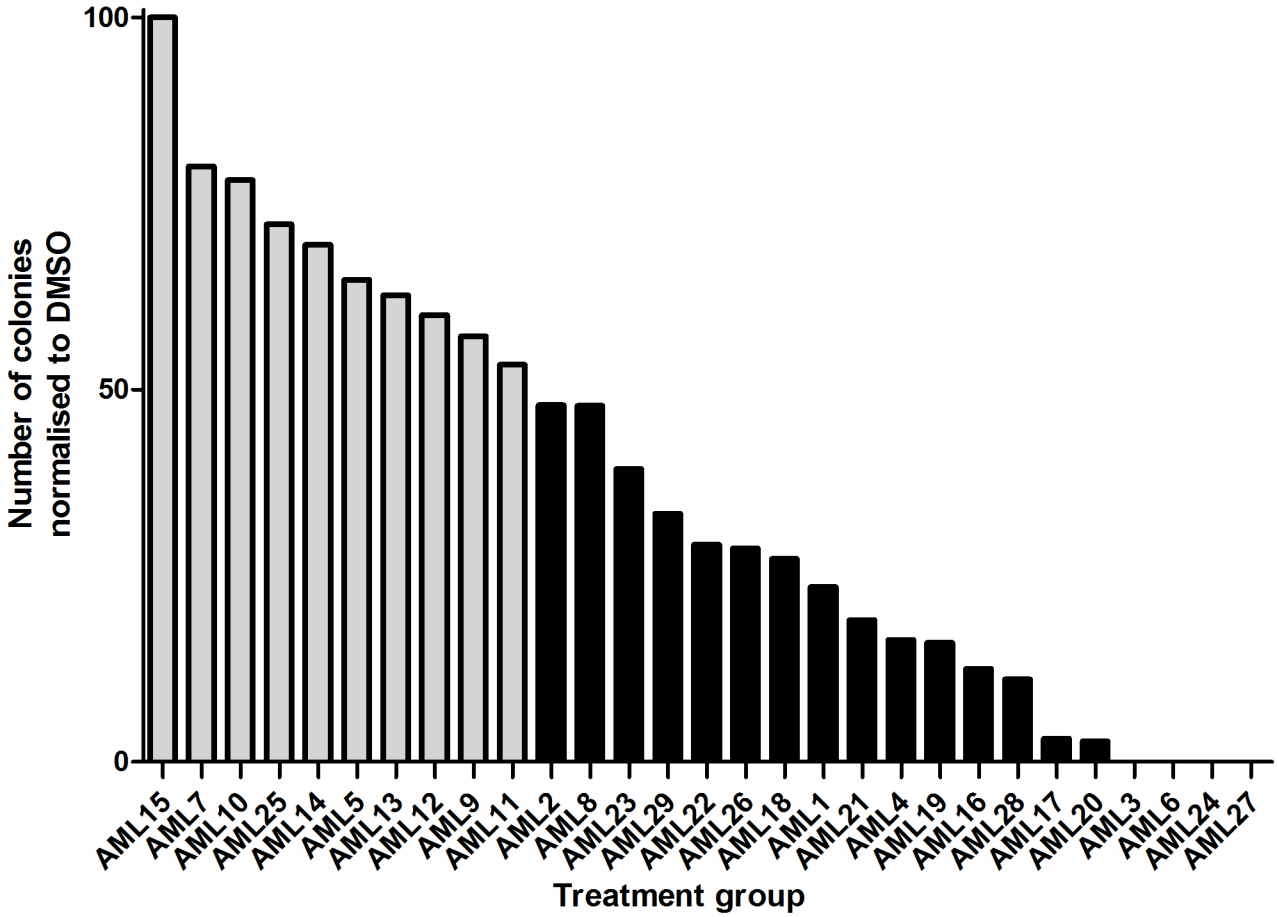

Patient	Age	Karyotype	Risk Group	Treatment type	Response to initial treatment	OS (days)	Dead/ Alive
AML1	79	46XX, i17(q)	Int-II	Pall	NA	78	D
AML2	68	46XX Add 11(p15)	Int-II	Cur	CR	1729	A
AML3	47	46XY	Int-I	Cur	CR	1660	A
AML4	64	46XY	Int-I	Pall	NA	124	D
AML5	50	46XY, t(15;17)	Favorable	Cur	CR	1848	A
AML6	24	46XY, inv(16)	Favorable	Cur	CR	1587	A
AML7	70	ND	NA	Pall	NA	282	D
AML8	78	46XY, 3q(26)	Adverse	Pall	NA	353	D
AML9	50	46XY, t(15;17)	Favorable	Cur	CR	1638	A
AML10	55	46XY, t(3;7)	Int-II	Cur	CR	334	D
AML11	63	Failed	NA	Cur	CR	1266	D
AML12	70	46XY	Int-I	Cur	CR	1896	D
AML13	82	Failed	NA	Pall	NA	593	A
AML14	44	46XX, +15	Int-II	Cur	CR	494	A
AML15	28	46XX, t(8;21)	Favorable	Cur	CR	195	A
AML16	67	Failed	NA	Cur	CR	421	A
AML17	55	46XX	Favorable	Cur	CR	51	A
AML18	53	46XX	Int-I	Cur	PR	88	A
AML19	44	46XY	Int-I	Cur	CR1noplt	209	A
AML20	20	46XY, Add 8(p21), MLL translocation	Adverse	Cur	CR	223	A
AML21	58	Complex (+6,add(10),t(11;19),+13,+ider(19),+21)	Adverse	Cur	REF	227	A
AML22	63	46XY, t(15;17), +8	Favorable	Cur	CR	211	A
AML23	55	Complex (-5q, -7q, -10q, -12p, -16, +11)	Adverse	Cur	REF	58	D
AML24	38	46XY	Favorable	Cur	CR1	271	A
AML25	65	46XX	Favorable	Cur	CR/MRD +	394	A
AML26	71	46XX	Int-I	Pall	NA	79	D
AML27	19	46XY	Int-I	Cur	CR	896	D
AML28	74	46XY	Int-I	Pall	NA	233	D
AML29	71	NA	NA	Pall	NA	9	A

Supplementary Table 1

Cell line	Oncogene/mutation
Kasumi-1	t(8;21) (AML1-ETO)
KG-1	FGFR1OP2-FGFR1 (OP2-FGFR1)
ME-1	inv(16)(p13q22) (CBFB-MYH11)
OCI-AML3	NPM1 (type A), DNMT3A (R882C)
HEL	JAK2 (V617F)
U937	t(10;11)(p13;q14) (CALM-AF10)
SKM-1	t(1;19)(q21;q13), del(2)(p11), del(9)(q12), p53 mutation
Nomo-1	t(9;11) (MLL-AF9)
MOLM-13	ins(11;9) (MLL-AF9)
K562	t (9;22), BCR-ABL (myeloid blast crisis)

Supplementary Table 2: Genes differentially expressed following treatment with C646

SYMBOL	KG1_logFC	KG1_adj_P_Val	Kasumi-1_logFC	Kasumi-1_adj_P_Val
ARRDC3	0.916669267	0.000038924	1.097139344	0.000156983
ASF1B	-0.953885608	0.000000148	-0.743984738	0.0000622
ATAD2	-0.623448874	0.000136843	-0.885614569	0.0000304
C11orf82	-0.755025048	0.00000224	-0.858766626	0.0000194
C1orf135	-0.787745006	0.00000257	-0.599849296	0.000284225
C5orf41	1.1281674	1.079E-07	0.60050232	0.000984683
C9orf142	-0.789650455	0.00000104	-0.71793558	0.000109381
CCNA2	-0.618657515	0.0000484	-0.909488767	0.0000128
CCNE2	-1.123527172	3.59E-08	-1.032784864	0.0000115
CD79B	0.606930175	0.0000241	0.783127924	0.000146752
CD96	0.739751323	0.00000903	0.633830926	0.000432111
CDC25A	-0.624478232	0.028574111	-0.723226621	0.00145612
CDC45L	-0.964077755	0.000000161	-1.032523434	0.00000901
CDCA2	-0.617468173	0.0000212	-0.665199886	0.000140938
CDCA5	-0.775666775	0.00000174	-0.980084316	0.00000932
CDKN3	-0.748802186	0.00000311	-0.729852177	0.0000538
CDT1	-1.019287274	9.08E-08	-0.62409966	0.002229886
CENPK	-0.662006163	0.0000113	-0.672160359	0.00012222
CENPM	-0.892907734	3.20767E-06	-0.904727411	1.85833E-05
CEP78	-0.59866638	0.000518203	-0.69720591	0.000362968
CHAF1A	-0.665761643	0.000121717	-0.80703793	0.0000223
CHAF1B	-0.65641296	0.0000251	-0.781334799	0.000068
CRELD2	-0.72612208	0.0000329	-0.687623722	0.0000675
DSCC1	-1.16175449	0.000000123	-0.813807581	0.0000415
DTL	-0.843770509	0.00000273	-0.949159737	0.0000128
E2F2	-1.011548346	0.000000446	-1.032686134	0.0000057
EVI2A	1.126276165	1.61E-08	0.833391216	0.0000772
EXO1	-0.78821822	0.000002799	-0.693236301	0.000766946
FAM149B1	0.753235786	0.0000035	0.618945983	0.000257581
FEN1	-0.872217692	5.915E-07	-0.948897738	0.00001834
FTHL12	1.251116736	0.000001316	0.680572611	0.005734735
FTHL16	0.981925966	0.000000161	0.745879611	0.0000439
FTHL7	0.999868659	0.000000394	0.645302713	0.000226147
FTHL8	1.40638593	0.000000869	0.679534862	0.004109704
GINS2	-0.87580594	0.000000385	-1.000885813	0.0000115
GINS3	-0.662728795	0.0000118	-0.844853379	0.0000181
GMNN	-0.605823576	0.0000303	-0.662281652	0.000199468
HAUS8	-0.653038768	0.000026735	-0.691902242	0.000228734
HELLS	-0.618301223	0.0000324	-0.770574971	0.000089439
HIST1H2BD	1.949849594	3.088E-10	0.647729751	0.029865014
HIST2H2AA3	0.714418315	0.000030823	0.638312369	0.000665218
KIAA0355	1.018677481	0.000000406	0.813118003	0.0000194
KIAA1147	0.770694176	0.00000376	0.762251759	0.0000287
KLHL24	1.083631381	0.000000158	0.770178777	0.000415095
KNTC1	-0.598659839	0.0000419	-0.743940783	0.0000697
LGALS1	0.832630148	0.00000093	0.627656476	0.000261548
LOC285741	0.749692364	0.00000344	0.771128188	0.000675036
LOC727803	-0.614222694	0.0000335	-0.591644383	0.000435301

LOC729816	-0.592789324	0.0000332	-0.678693377	0.0000697
LOC88523	1.111487192	0.000000249	0.836889185	0.0000323
LSM4	-0.989625664	0.000000188	-0.668346197	0.000359092
MAGED2	0.779049135	0.000551016	0.6472256	0.047739775
MCM10	-0.923315633	2.0565E-06	-0.976252902	0.0000198
MCM3	-0.619729533	0.0000275	-0.716738686	0.000096384
MCM4	-0.949808391	4.185E-07	-0.882847867	0.00004315
MCM5	-0.987629332	0.000000417	-0.889471957	0.0000931
MXD4	0.858634402	0.00000175	0.608226775	0.000166318
NDRG1	1.471437357	7.83E-09	0.823287374	0.0000308
NR2C2AP	-0.597703289	0.0000822	-0.648300506	0.000870524
NUP210	-0.668061962	0.0000433	-0.645356167	0.000216516
PCMTD2	0.613096672	0.0000164	0.664412109	0.000115841
PCNA	-0.688150445	0.00001253	-0.646374793	0.001004518
POLA2	-0.685846663	0.0000129	-0.790667946	0.0000733
PREPL	0.773168631	0.000003545	0.837726834	6.75635E-05
RAD54L	-0.684130868	0.00000771	-0.930746979	0.0000115
RANBP1	-0.61794029	0.00003846	-0.676119831	0.000180219
RECQL4	-0.720110296	0.00000326	-0.627704124	0.000393538
RRM2	-0.951959921	0.00000015	-1.174205246	0.00000171
RTKN	0.69511696	0.00000813	0.593437778	0.000408233
SGOL2	-0.638624556	0.0000833	-0.587710411	0.000589648
SIVA1	-0.739224143	0.000004925	-0.723227123	0.000226945
SLC38A2	0.649368543	0.00000978	0.615528331	0.000435301
SPC24	-0.621901008	0.0000233	-0.690399348	0.00024524
STAT2	0.721774826	0.00000771	0.698538824	0.0000515
TAGLN2	-0.771249068	0.00000725	-0.598086111	0.000979334
TK1	-0.699053194	0.0000269	-0.818048587	0.0000382
TM6SF1	0.71495505	0.0000117	0.718206838	0.0000585
TRIP13	-0.690147595	0.00000718	-0.980248801	0.00000905
TSC22D1	0.938624888	0.000944161	0.78907195	0.000172091
TYMS	-0.65434577	0.000034	-0.965553609	0.0000137
UBA7	0.697934803	0.0000175	0.616557429	0.000169767
UBE2T	-0.74704477	0.0000031	-0.693205874	0.0000592
UCK2	-0.612422961	0.000089	-0.674900587	0.0000622
UHRF1	-0.708695644	0.000113133	-0.774944635	0.000166918
UNG	-0.647507134	0.00005605	-0.612738019	0.000362821
XRCC3	-0.7715007	0.00000686	-0.630800997	0.00014753
ZNF442	0.899921834	0.00000425	0.63020026	0.00040197

* Genes highlighted in grey are direct p300 targets (data mined from the ENCODE project)